Shape Coexistence in the proton unbound ^{177}Au

Fuad Arif Ali

University of Guelph

Permanent address: College of Education, Department of Physics, University of Sulaimani, KRG-Iraq.

2017 CAP Congress, May 29 - June 2, Queen's University, Kingston, ON

Outlines:

- Introduction
- Laboratory Overview
  - Experimental Set-up (JUROGAMII -RITU - GREAT)
- Recoil-Decay-Tagging Technique
- Data Analysis of ^{177}Au
- Conclusion

Introduction:

- ~3000 unique ensembles of (p,n).
- Structure of exotic nuclei at the extremes of the nuclear landscape.
- Relative locations of single-particle orbitals near the drip line through the study of single-proton excitations through the phenomenon of shape coexistence in ^{177}Au.

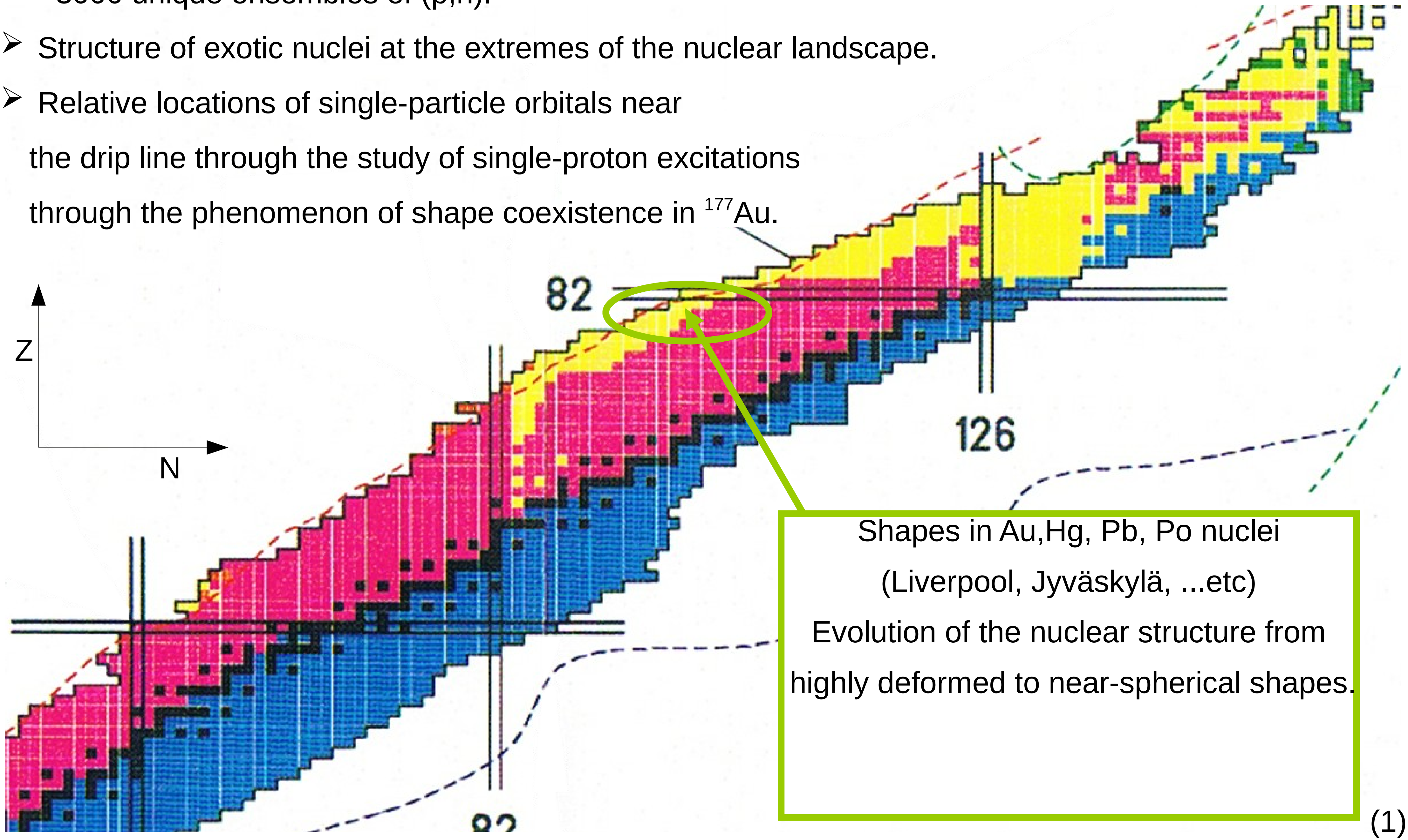

Shapes in Au,Hg, Pb, Po nuclei

(Liverpool, Jyväskylä, ...etc)

Evolution of the nuclear structure from highly deformed to near-spherical shapes.

(1)

Introduction:

- Shape coexistence refers to the phenomenon where two or more nuclear shapes that are based on different underlying configurations lie at very similar (usually low) excitation energies.

- Coexisting structures are sensitive to the interplay between the stabilizing presence of shell gaps and the deformation driving tendencies of residual interactions between single-particle orbitals.

- An intuitive interpretation of shape coexistence arises from the consideration of specific configurations based on multiple particle-hole (mp-nh) excitations across closed shells, which provide the basis for low-lying collective bands.

- Spherical, oblate and prolate minima are indicated in ^{186}Pb.

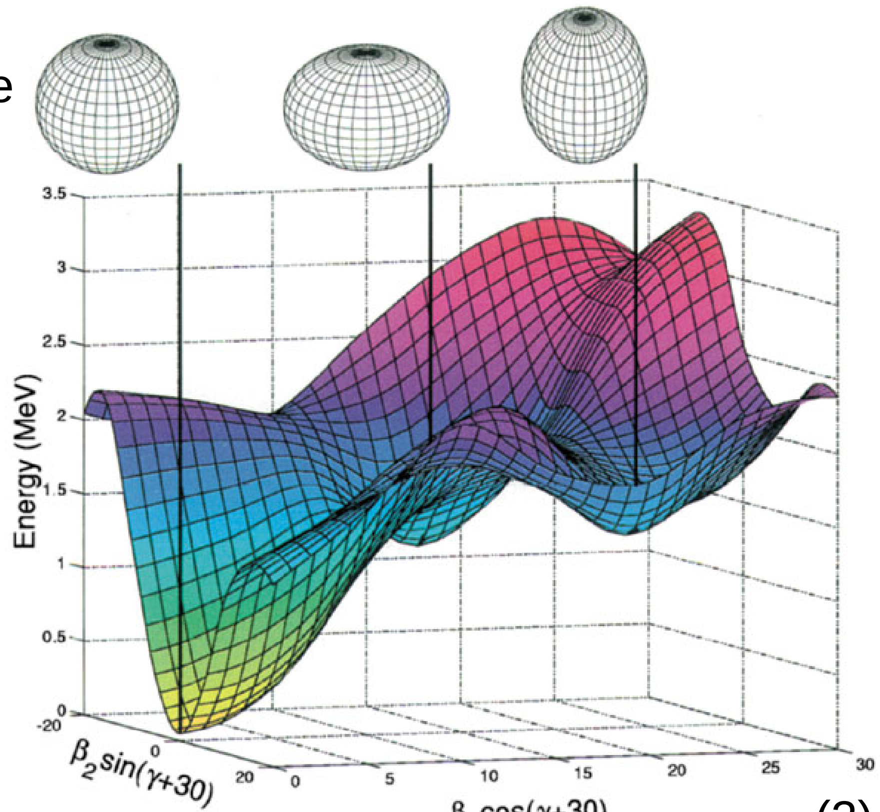

J. L. Wood *et al.*, Phys. Rev. C 14, 682 (1976).

Introduction:

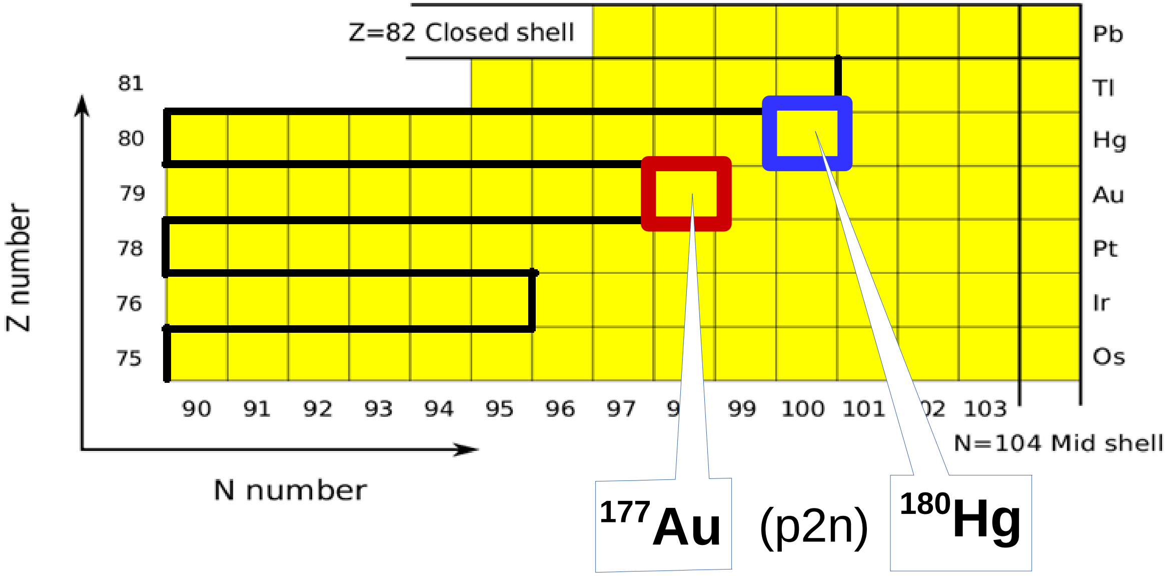

- Fusion-Evaporation-Reaction.
- Odd-A nuclei has more complicated excitation spectra .. .

  - low cross sections -> experimentally challenging, severe competition from fission and small evaporated-residues fragmented over many channels.

- Most extensively characterized regions of low-energy shape coexistence.
- An odd-proton about the $\boldsymbol{s}_{1/2}$, $\boldsymbol{d}_{3/2}$ and $\boldsymbol{h}_{11/2}$ orbitals below the shell gap and the $\boldsymbol{h}_{9/2}$, $\boldsymbol{f}_{7/2}$ and $\boldsymbol{i}_{13/2}$ intruder states above it.
  - Search for collective bands associated with
  - $\boldsymbol{h}_{9/2}$ and $\boldsymbol{f}_{7/2}$ intruder configurations
  - $\boldsymbol{s}_{1/2}$, $\boldsymbol{d}_{3/2}$ and $\boldsymbol{h}_{11/2}$ proton hole structures.

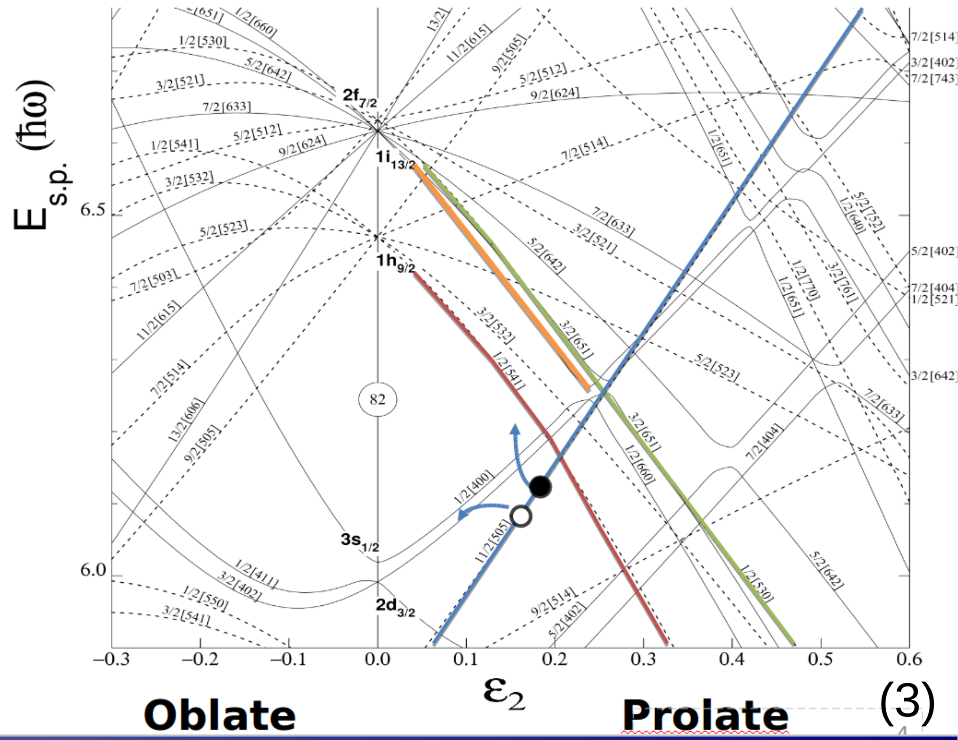

(3)

Proton-Hole and Proton-Particle configurations:

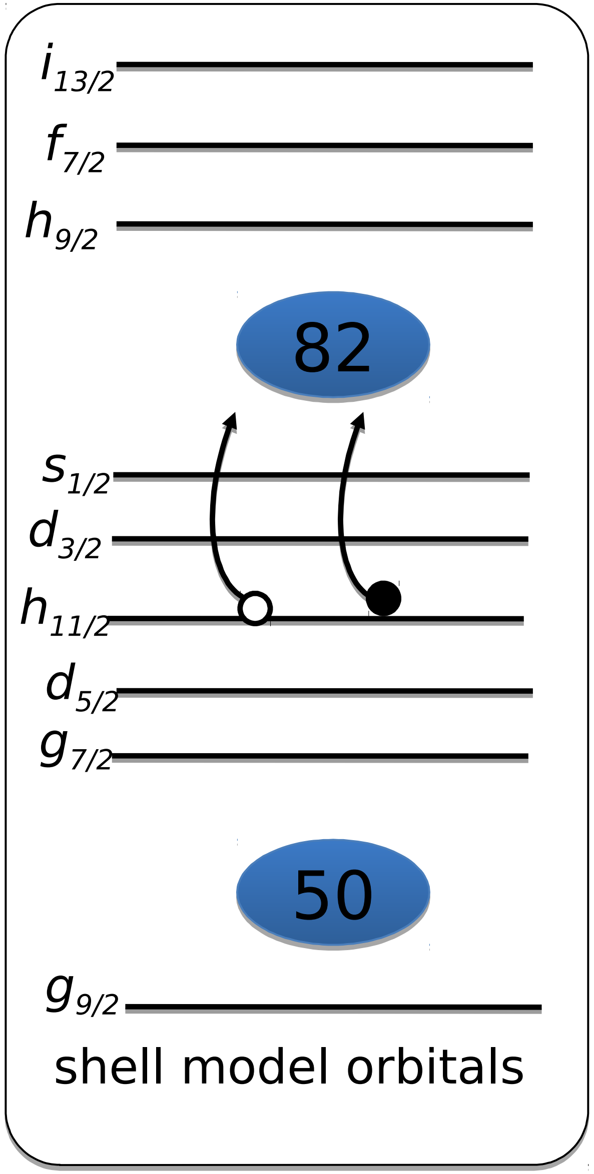

Hg 178
255 ms

\-

hole states
$s_{1/2}$, $d_{3/2}$, $h_{11/2}$

=

Au 177
1.230 ms

=

particle states
$h_{9/2}$, $f_{7/2}$, $i_{13/2}$

\+

Pt 176
6330 ms

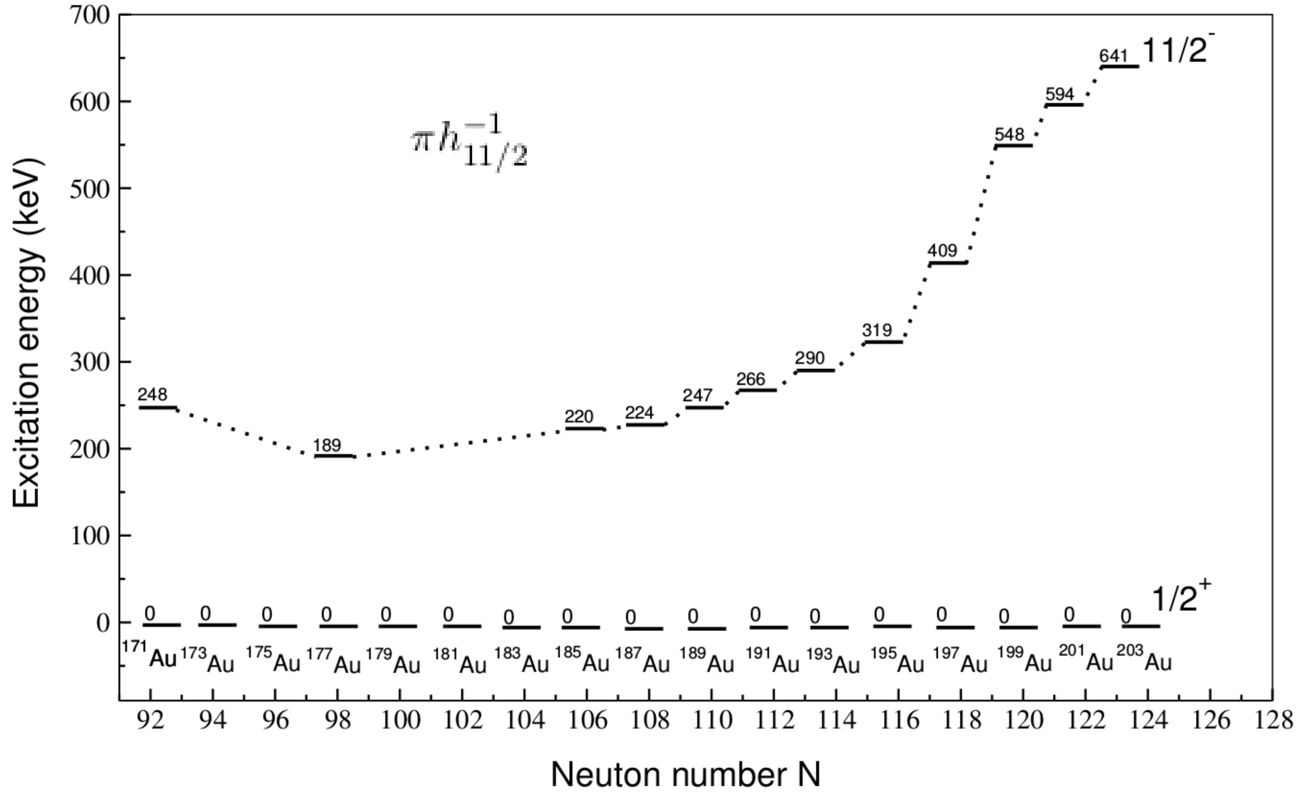

- Reduced valence space as the N = 126 closed shell is approached.
- Gap is sufficiently narrow ⇨ coexisting configurations to be built on proton excitations across the closed shell.
- 1p-4h can be formed.

Laboratory Overview (Experimental set up)

Laboratory Overview:

Experimental setup sketch:

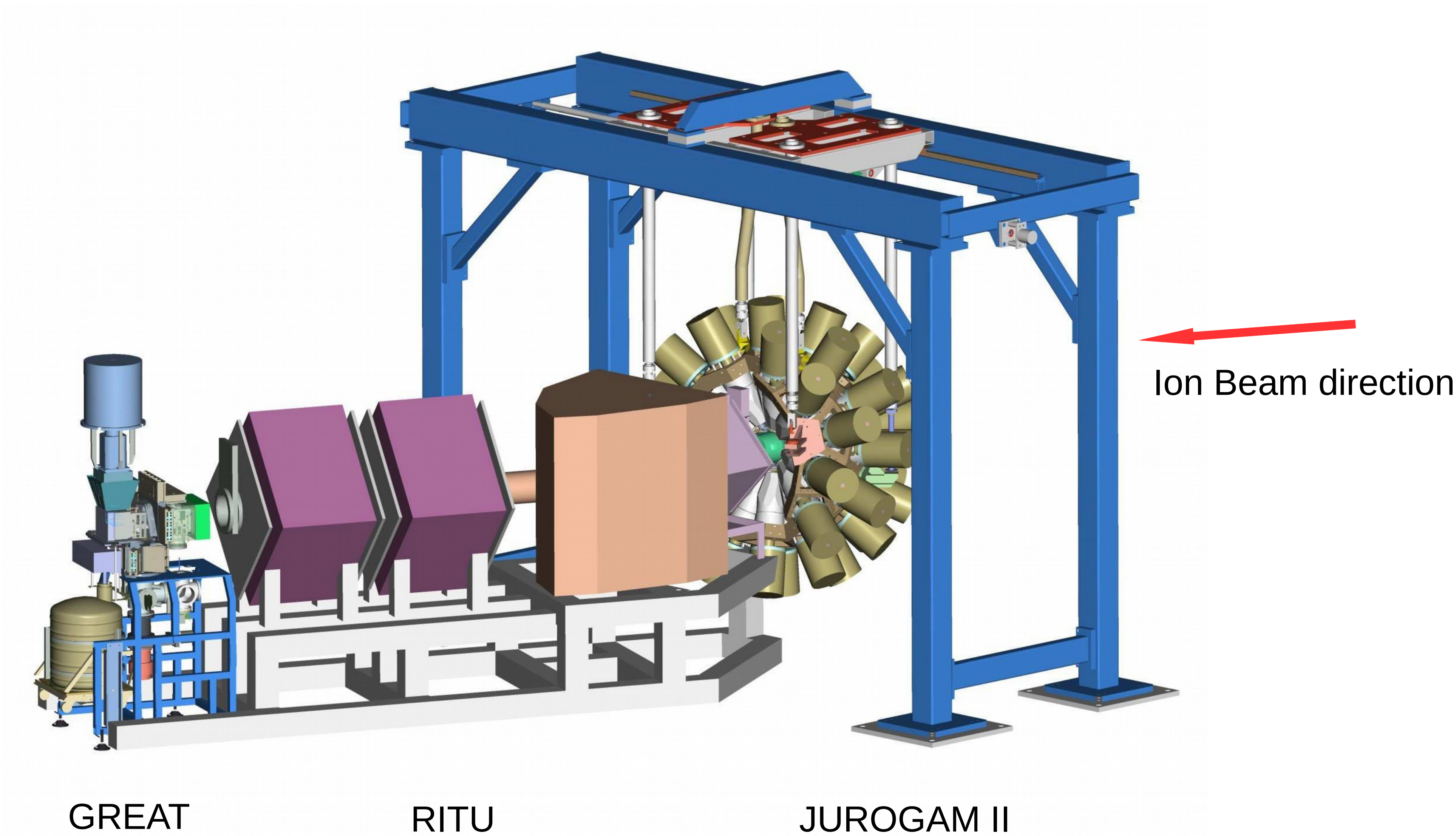

Experimental Setup: $^{88}Sr+^{92}Mo=^{180}Hg^*$ (at 378 MeV.):

RITU (Recoil Ion Transport Unit)

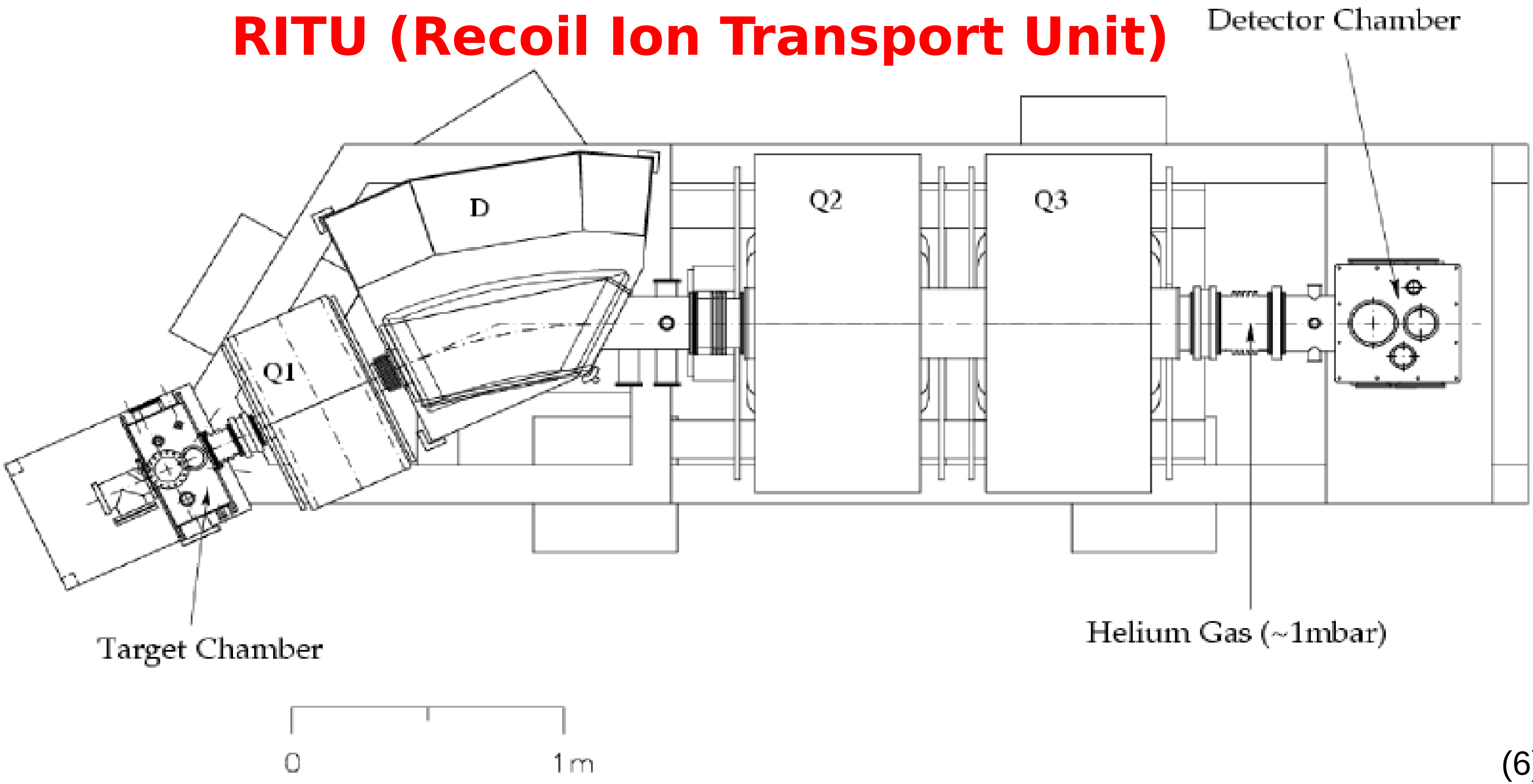

Experimental Setup: $^{88}Sr + ^{92}Mo = ^{180}Hg^*$ (at 378 MeV.):

RITU (Recoil Ion Transport Unit)

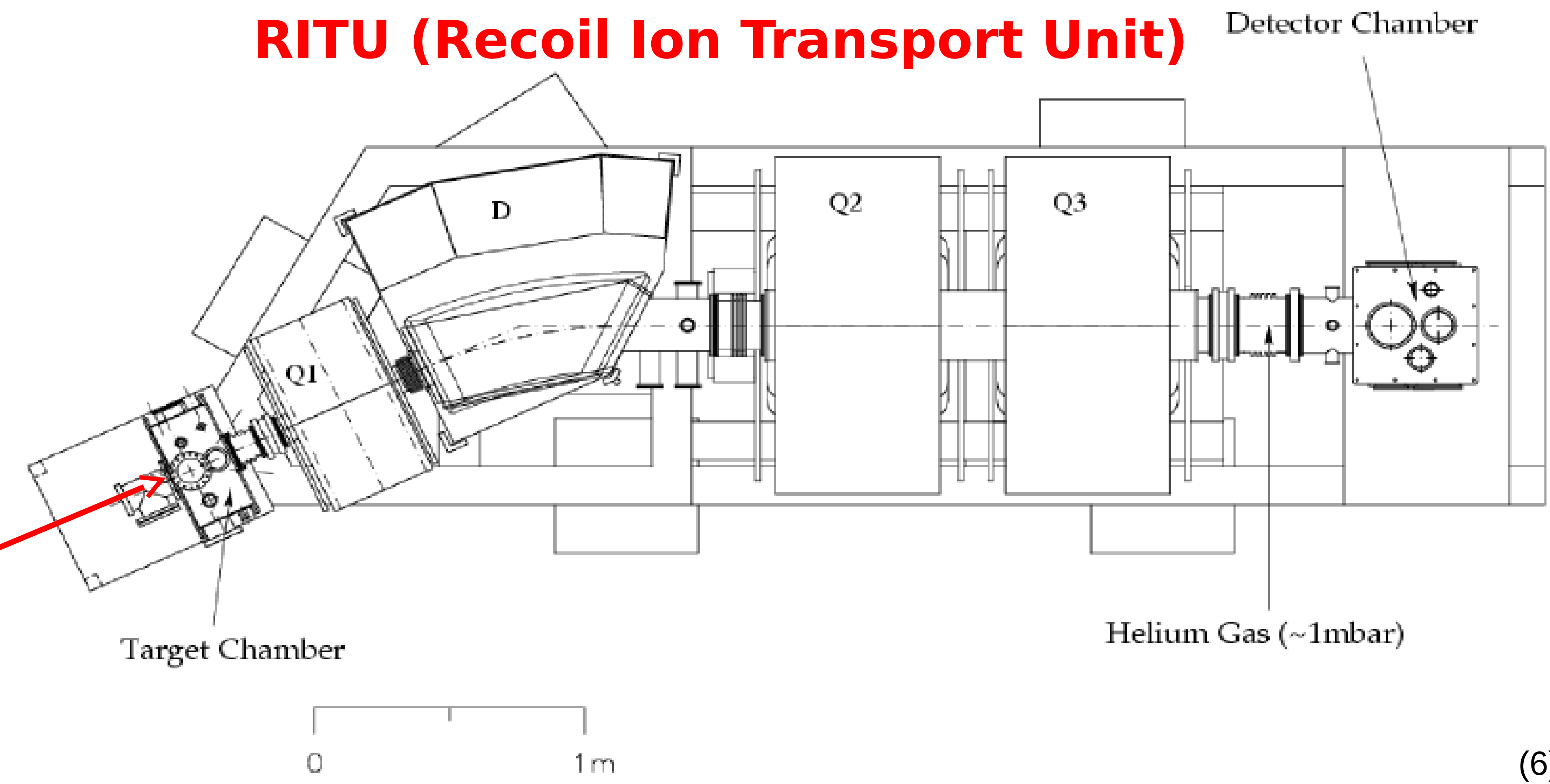

Experimental Setup: $^{88}Sr+^{92}Mo=^{180}Hg^{*}$ (at 378 MeV.):

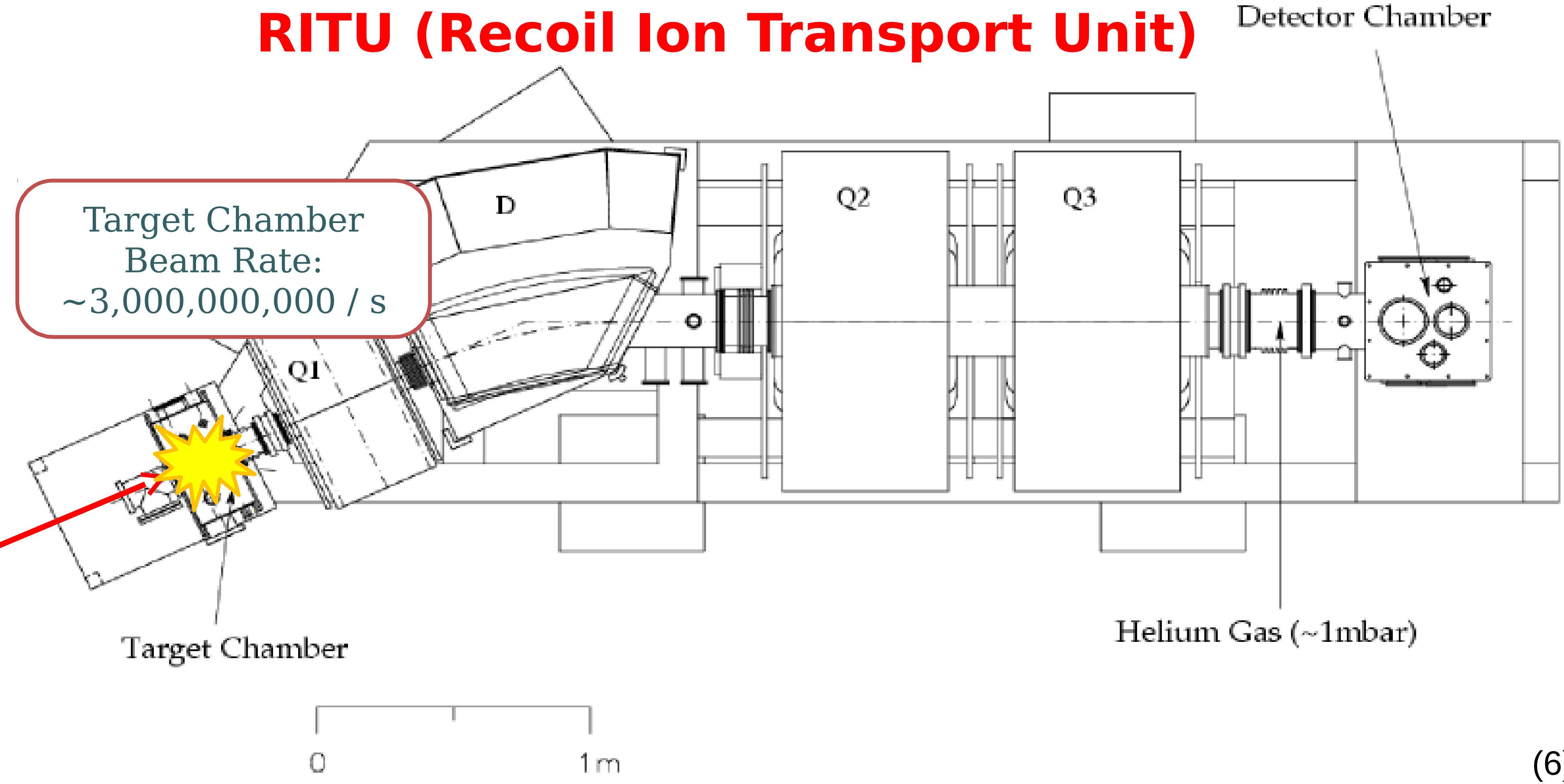

Experimental Setup: $^{88}Sr+^{92}Mo=^{180}Hg^*$ (at 378 MeV.):

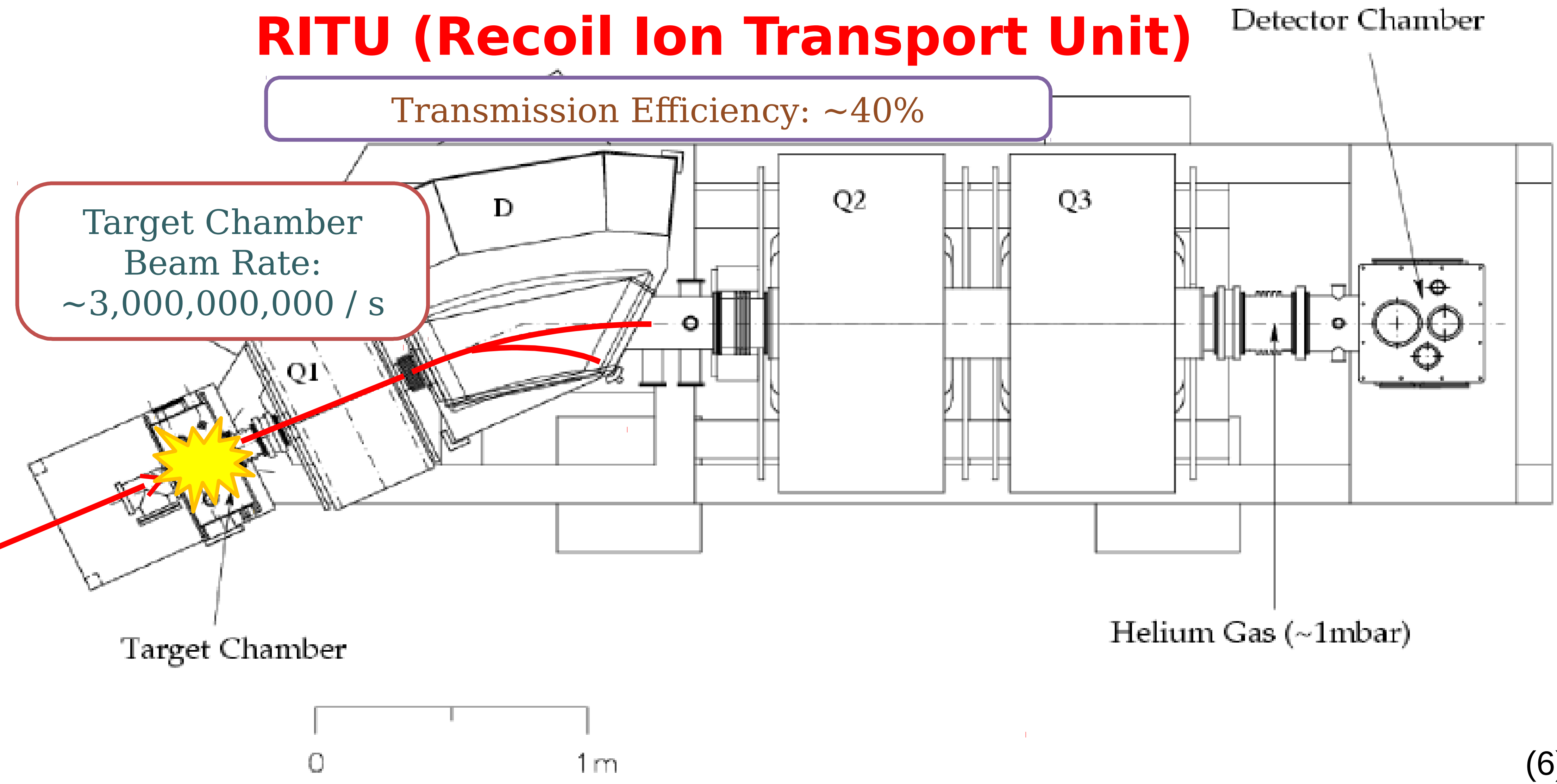

Experimental Setup: $^{88}Sr+^{92}Mo=^{180}Hg^*$ (at 378 MeV.):

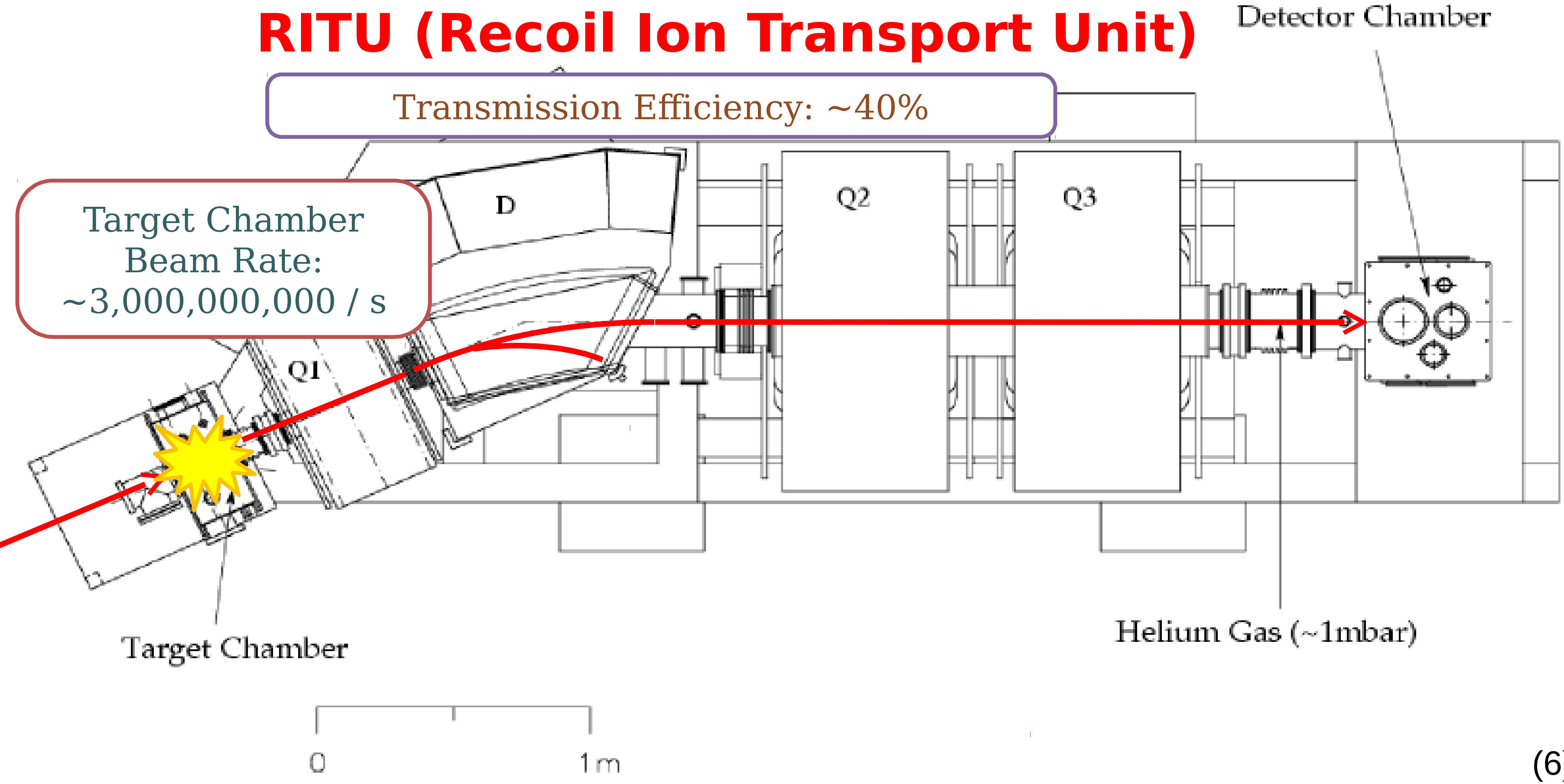

Experimental Setup: $^{88}Sr + ^{92}Mo = ^{180}Hg^*$ (at 378 MeV.):

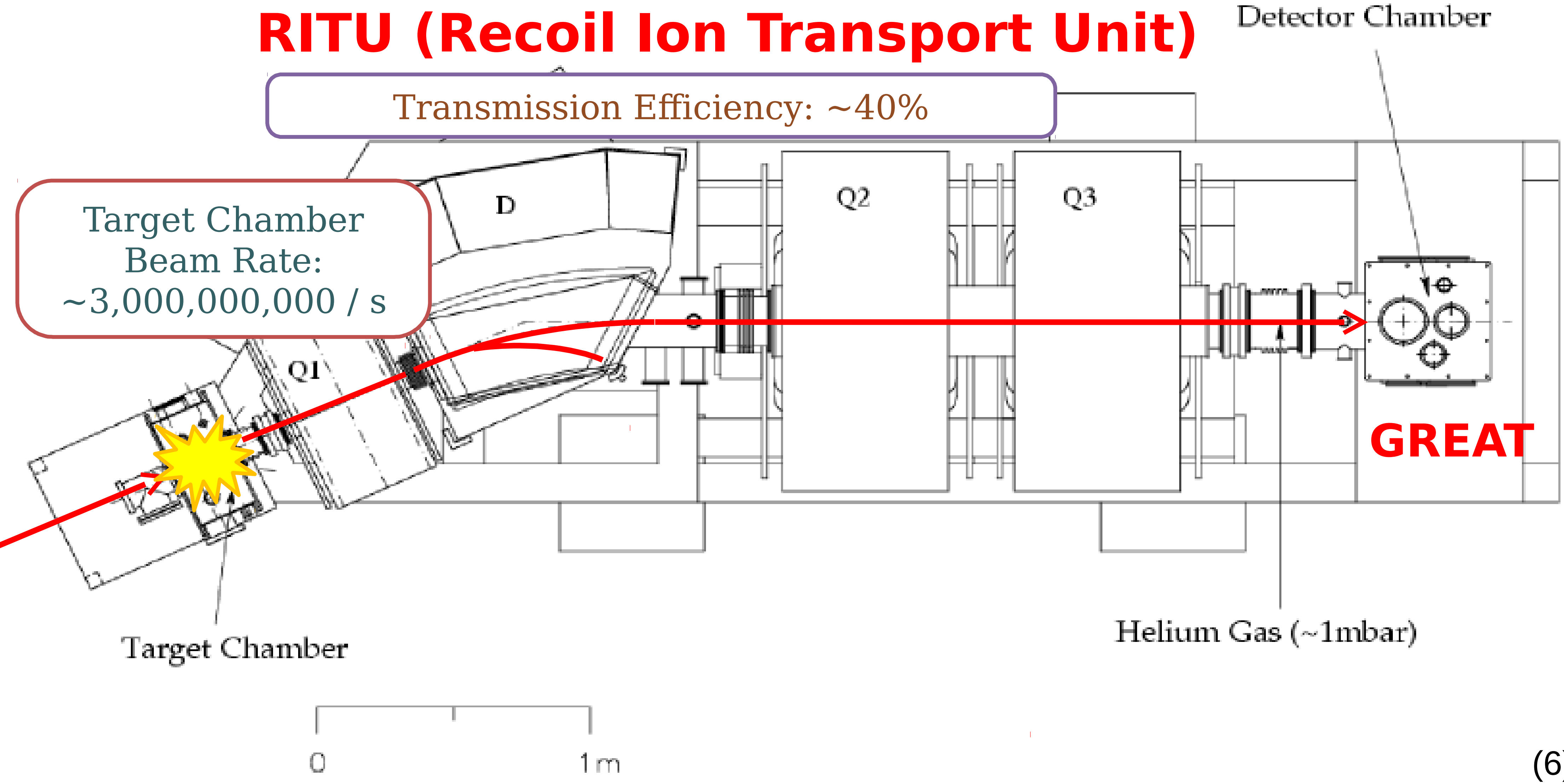

Experimental Setup: $^{88}Sr+^{92}Mo=^{180}Hg^*$ (at 378 MeV.):

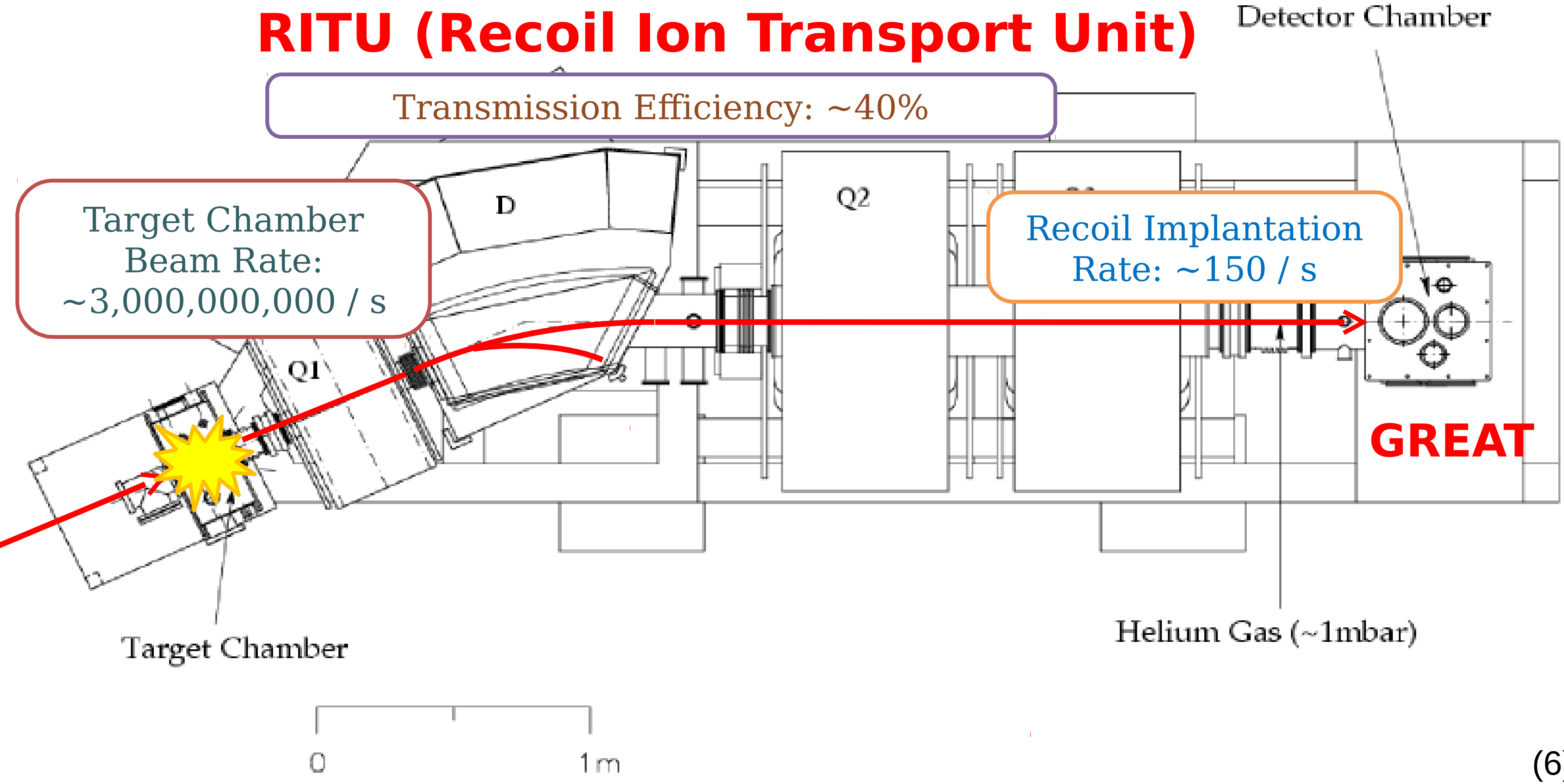

Experimental Setup: $^{88}Sr + ^{92}Mo = ^{180}Hg^*$ (at 378 MeV.):

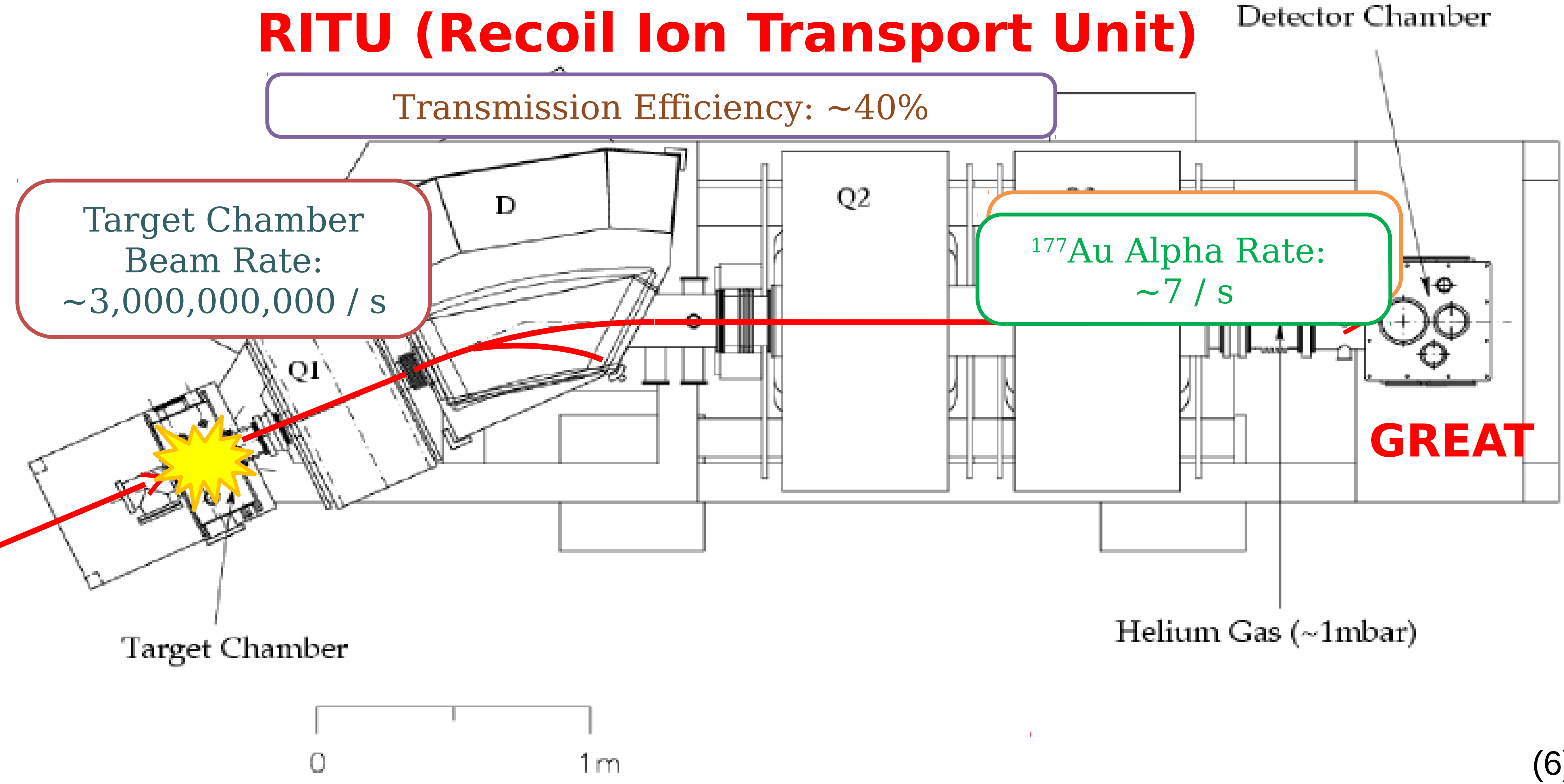

Experimental Setup: $^{88}Sr+^{92}Mo=^{180}Hg^*$ (at 378 MeV.):

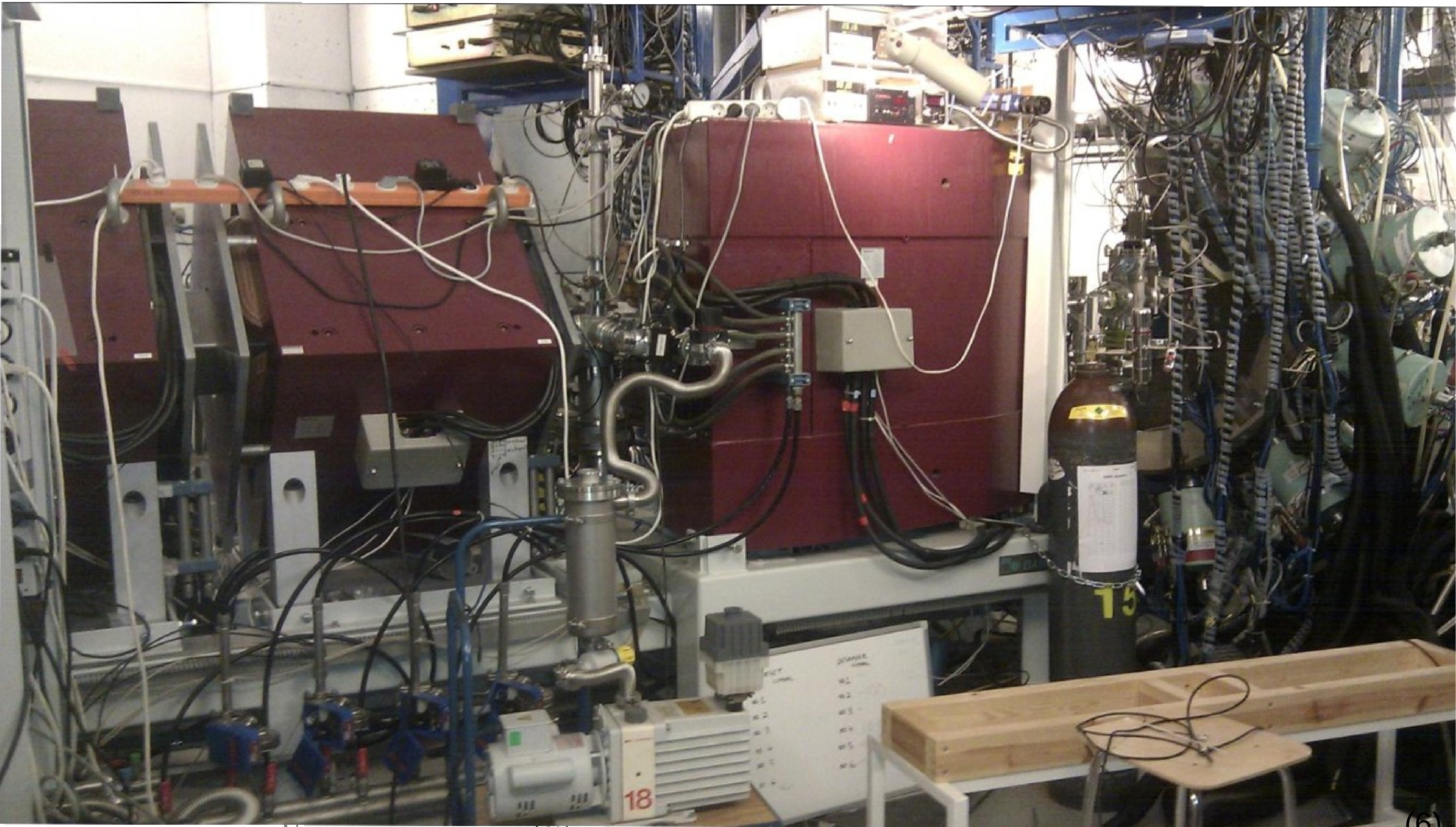

The JUROGAMII and DSSD:

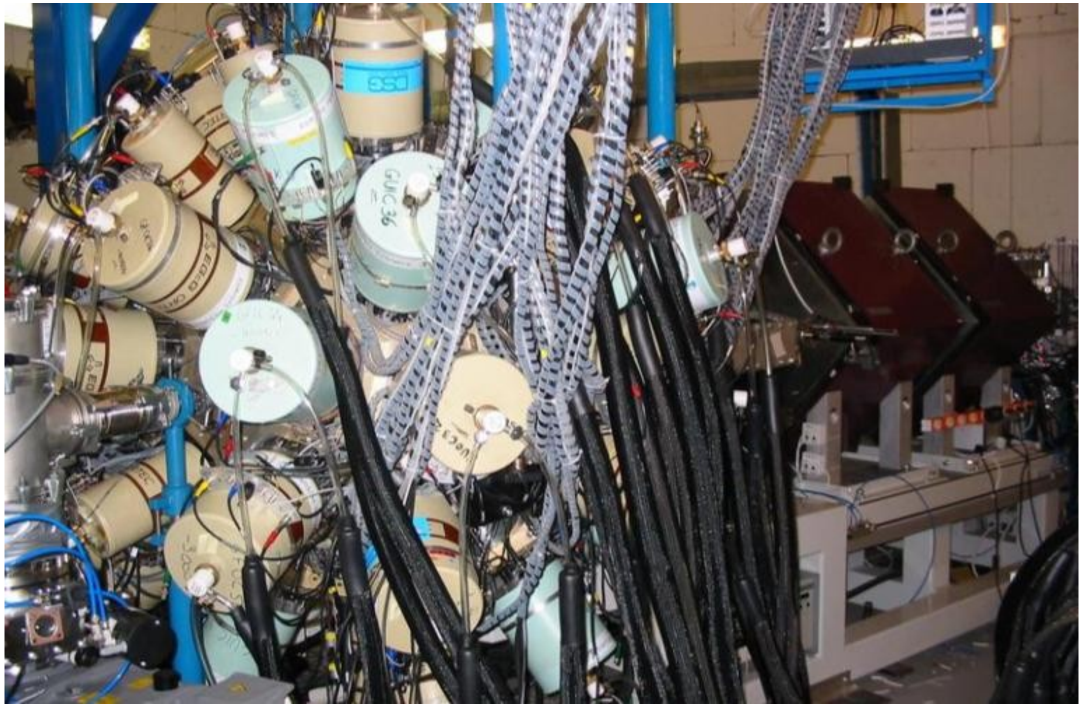

Double Sided Silicon Strip Detector (DSSD)
Measures energies of charged particles (recoils, alphas, electrons and protons).
40 vertical strips.
2 sides of 60 horizontal strips.
4800 pixels in the detector.

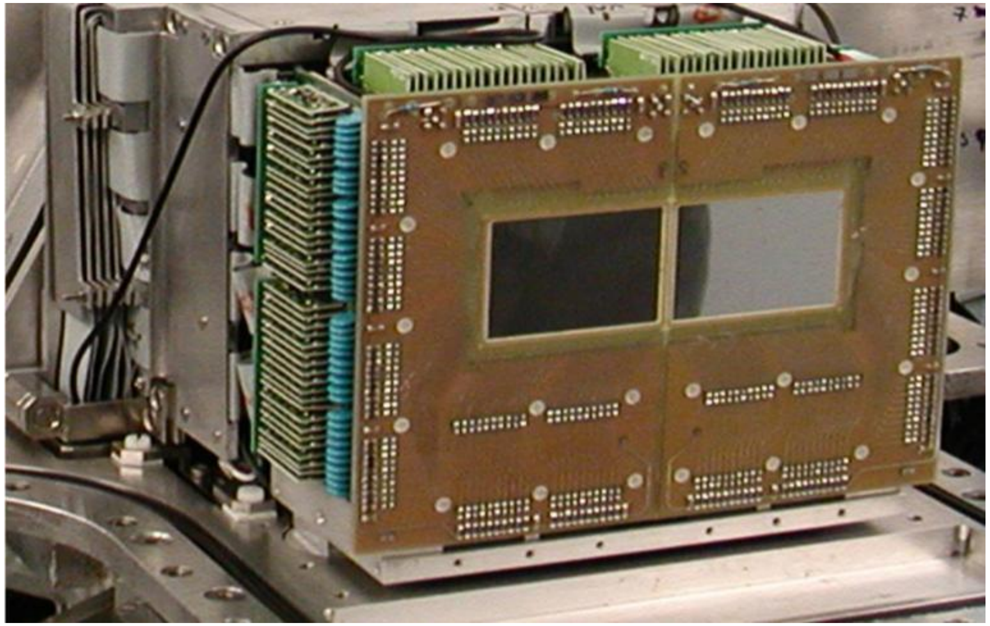

Compton suppressed hyper-pure germanium detector array JUROGAM II
Sensitive to photons in the region: 50keV < E_g < 2MeV.
24 segmented CLOVER detectors.
10 PHASE I detectors.

GREAT Spectrometer:

The planar germanium detector is located ~1cm behind the DSSD and a 0.5mm thick Be entrance window.

Sensitive to photons in the region: 10keV < E_g < 400keV, and up to several MeV for electrons.

12 vertical strips.

24 horizontal strips.

288 pixels in the detector.

Crystal size:
130 mm x 70 mm x 15 mm

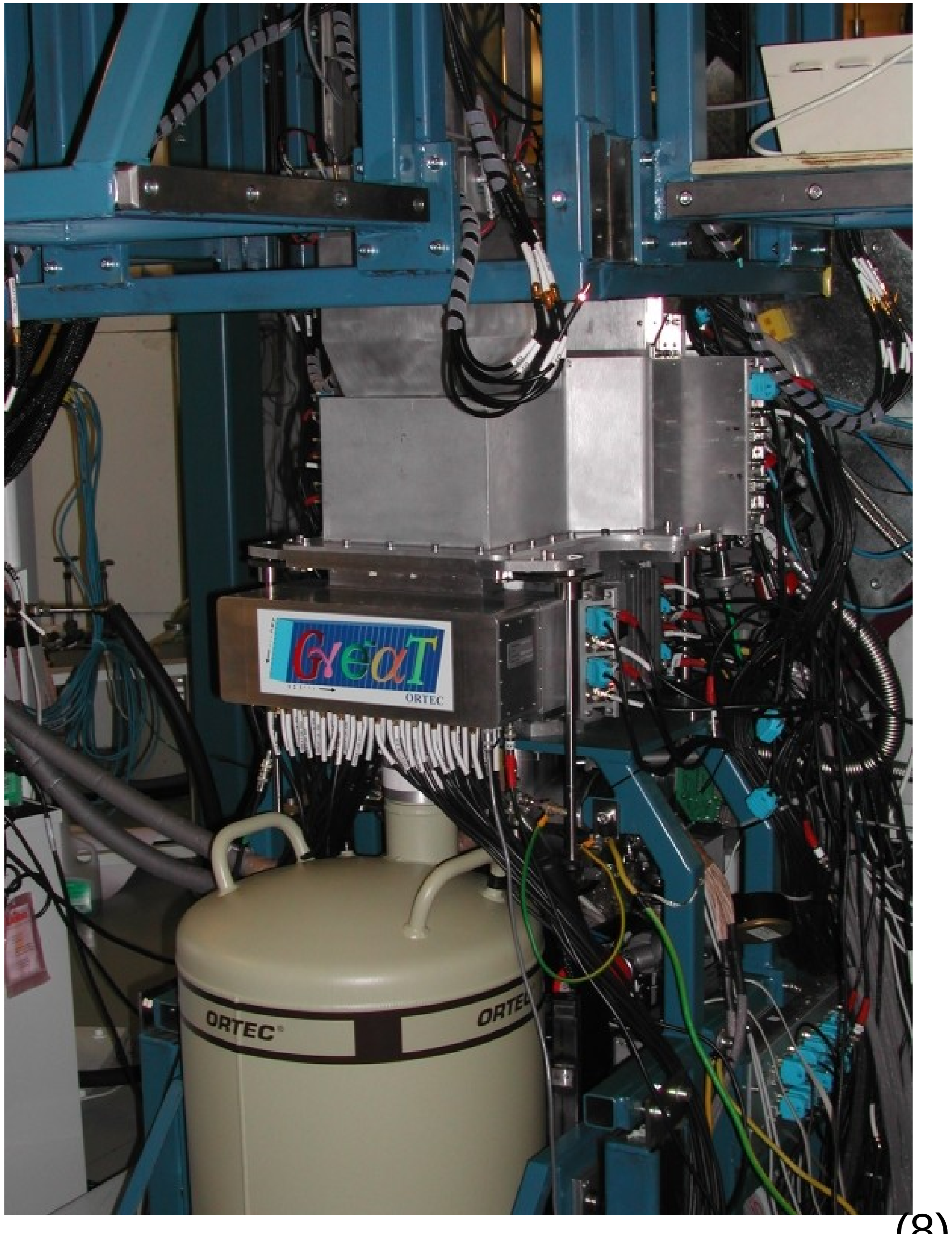

(8)

Recoil Decay Tagging Technique (RDT)

Recoil Decay Tagging Technique:

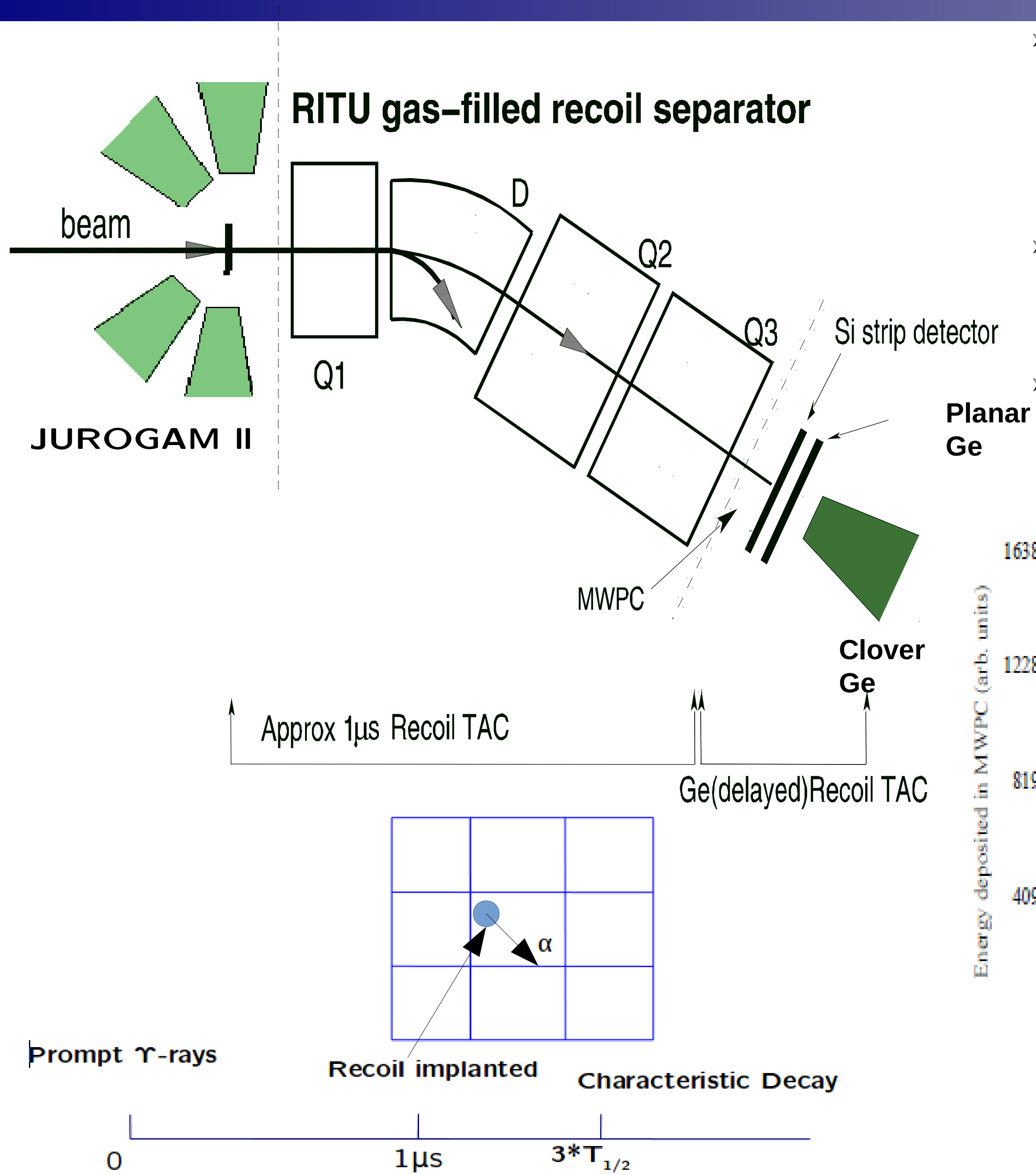

- Correlating of prompt gamma-rays at the target position with recoil and their subsequent alpha decay at the focal plane.
- Distinguish between recoil and scattered beam implantation in the DSSD.
- Z number and velocity ensure this discrimination.

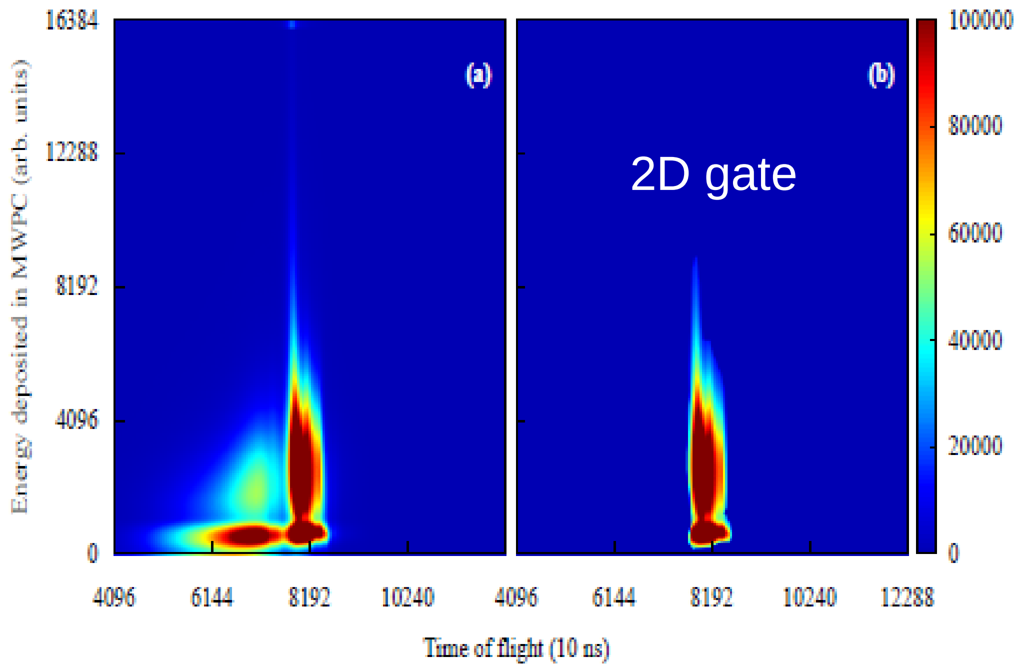

Tof Flight vs. dE Deposited in MWPC

Recoil Decay Tagging Technique:

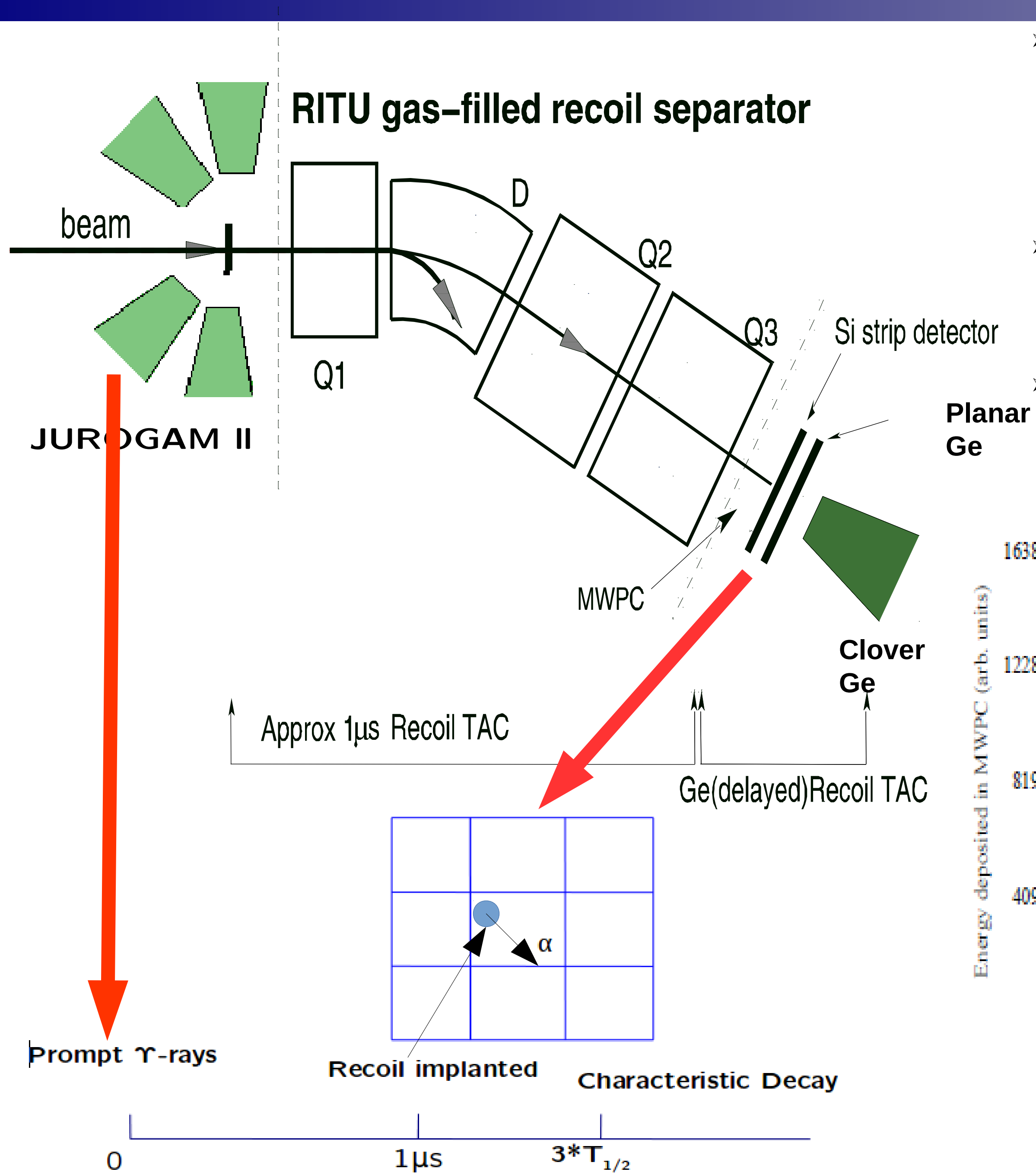

- Correlating of prompt gamma-rays at the target position with recoil and their subsequent alpha decay at the focal plane.
- Distinguish between recoil and scattered beam implantation in the DSSD.
- Z number and velocity ensure this discrimination.

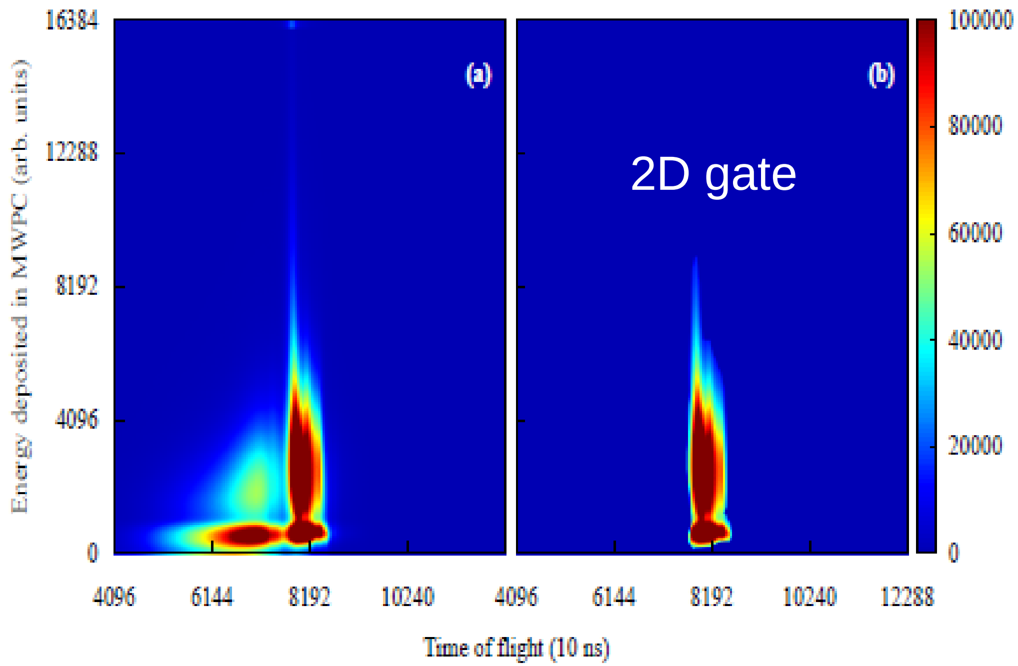

Tof Flight vs. dE Deposited in MWPC

In-Beam gamma-ray Spectroscopy of ^{177}Au :

- ^{177}Au and recoils from other reaction channels. γ-rays in coincidence with any recoil.

- γ-rays by recoil followed by a characteristic alpha decays of ^{177}Au. The transition are belong to ^{177}Au only.

- Gamma-gating: γ-rays observed in that band which are coincidence with 257keV.

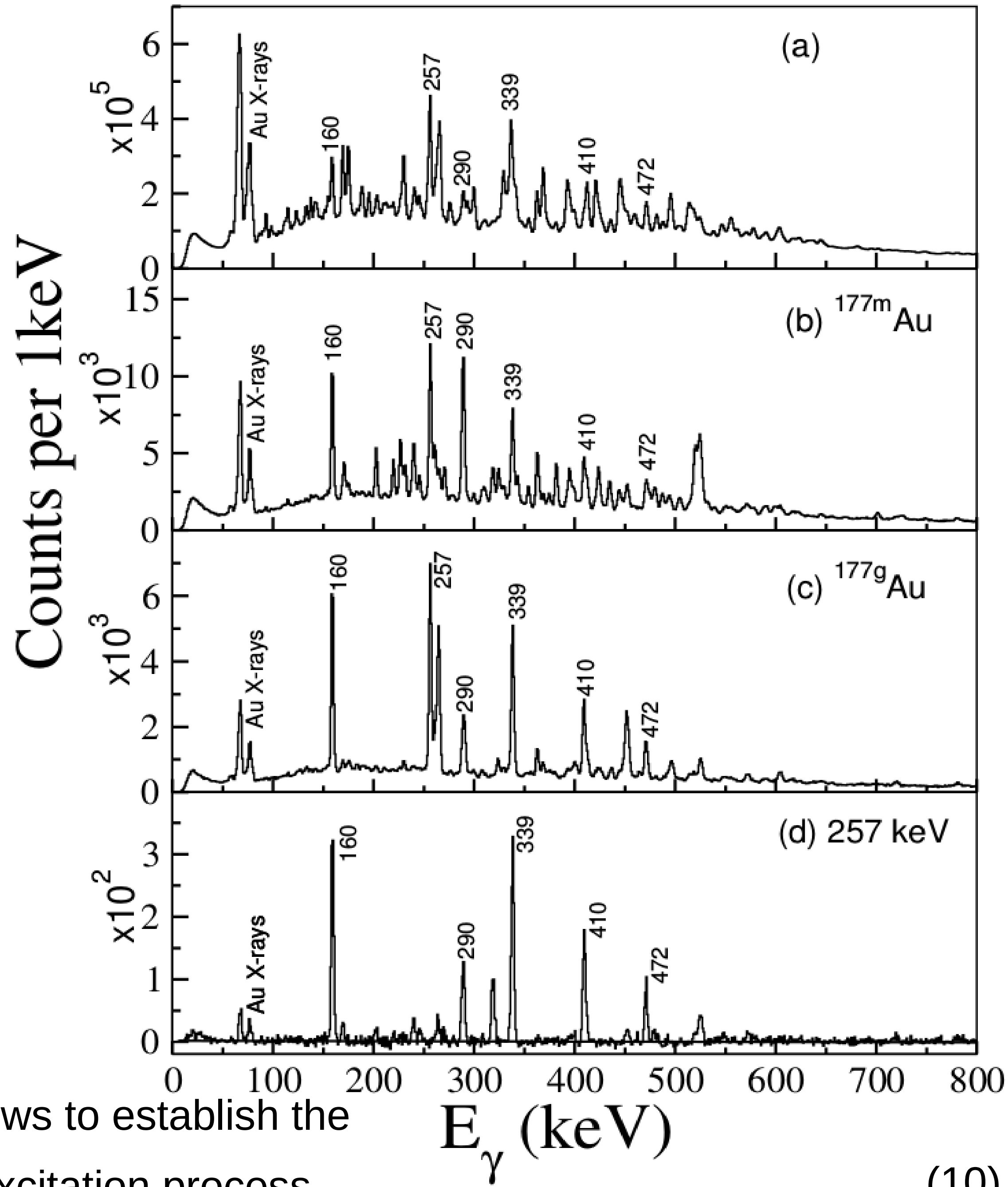

Recoil-decay tagged γ−γ coincidence matrices allows to establish the relationships between γ rays populated in the de-excitation process.

Experimental Results and its Interpretations

What previously known on ^{177}Au:

- ^{177}Au was first observed by Siivola who identified the 6115 keV α decay from the 11/2 − state. at Berkeley in 1968
- First insight into the higher-spin excited states, (GAMMASPHERE).
- α decay spectroscopy of ^{183}Tl and ^{181}Tl,
- Recent laser spectroscopy measurements confirmed the g.s and isomer spins to be 1/2 + and 11/2- .

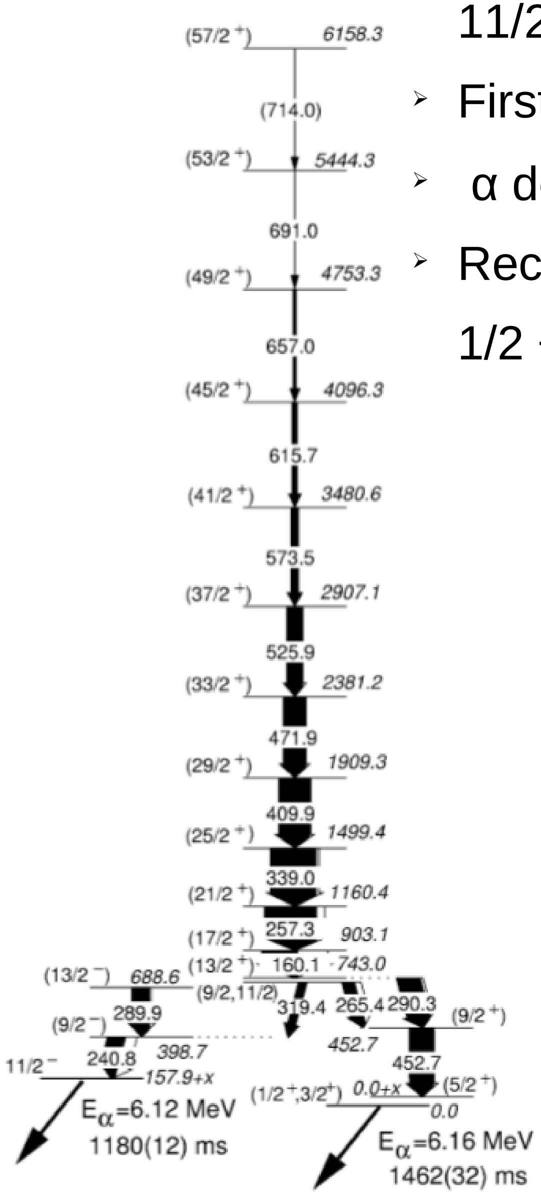

F.G. Kondev et al; Phys. Lett. **B**, 268 (2001)

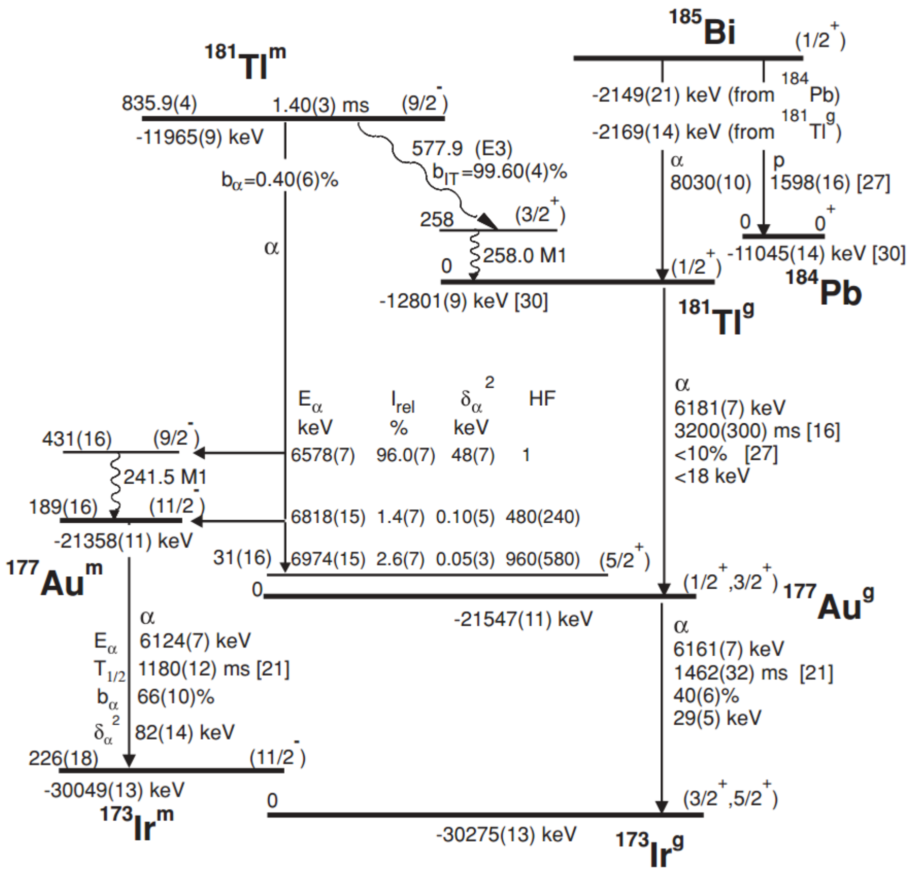

A. N. Andreyev, et al; PhyRev C **80**, 024302 (2009)

The α-decaying states in ^{177}Au:

- A precise measurement on T_1/2 and Energy of the alpha decaying:
- α particles that are observed up to 3900 ms after a recoil implantation in same DSSD pixel.

The centroids of α decays are distinct, however peak shapes overlap:

Leads to an effect on half-lives measurement .

- To suppress the background arising from correlation with overlapping decay.
- Exclusive gamma-ray feeds used.

 Some level of suppression is apparent

- Unique gamma-ray to a specific nucleus.

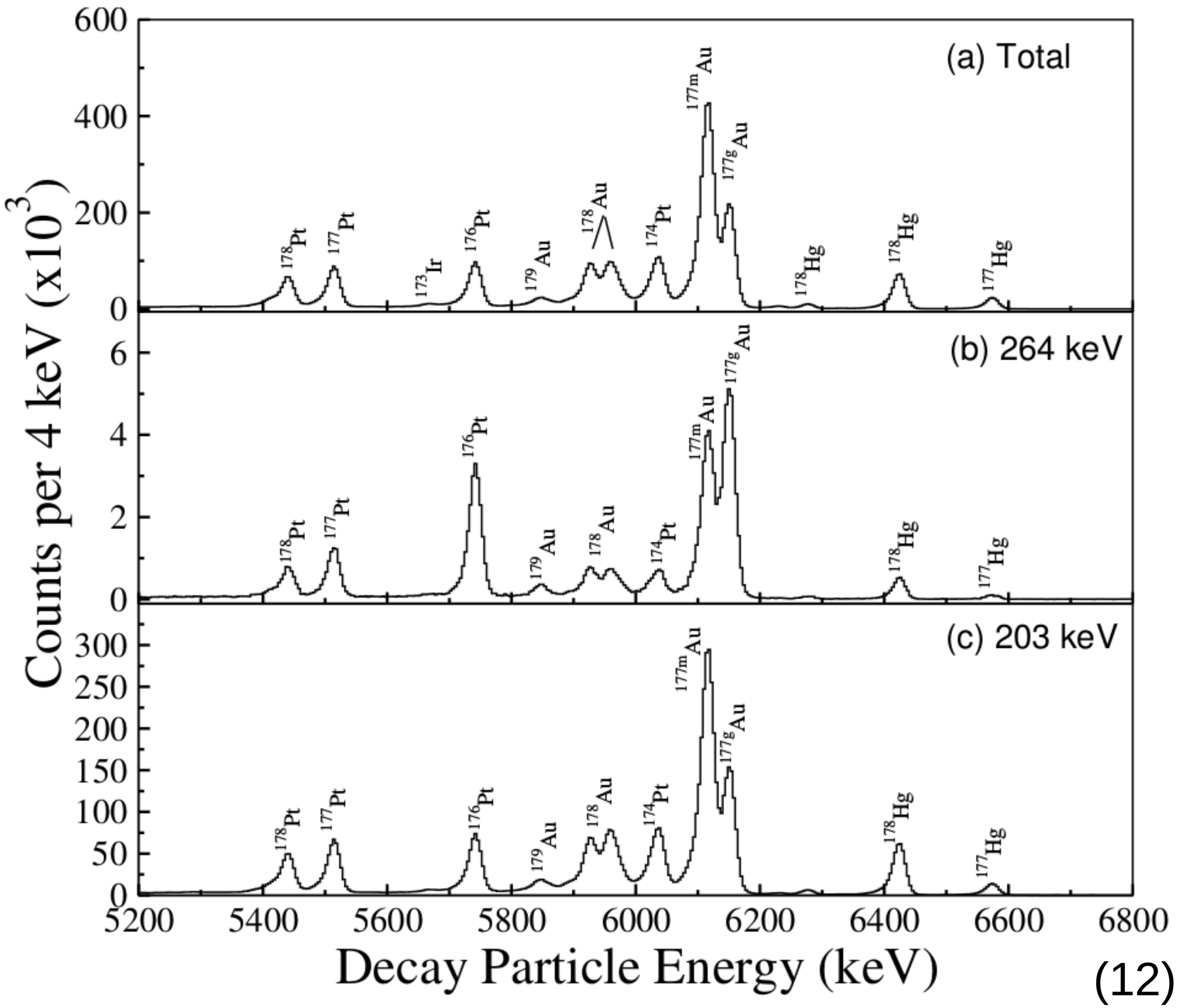

(12)

The α-decaying states in ^{177}Au:

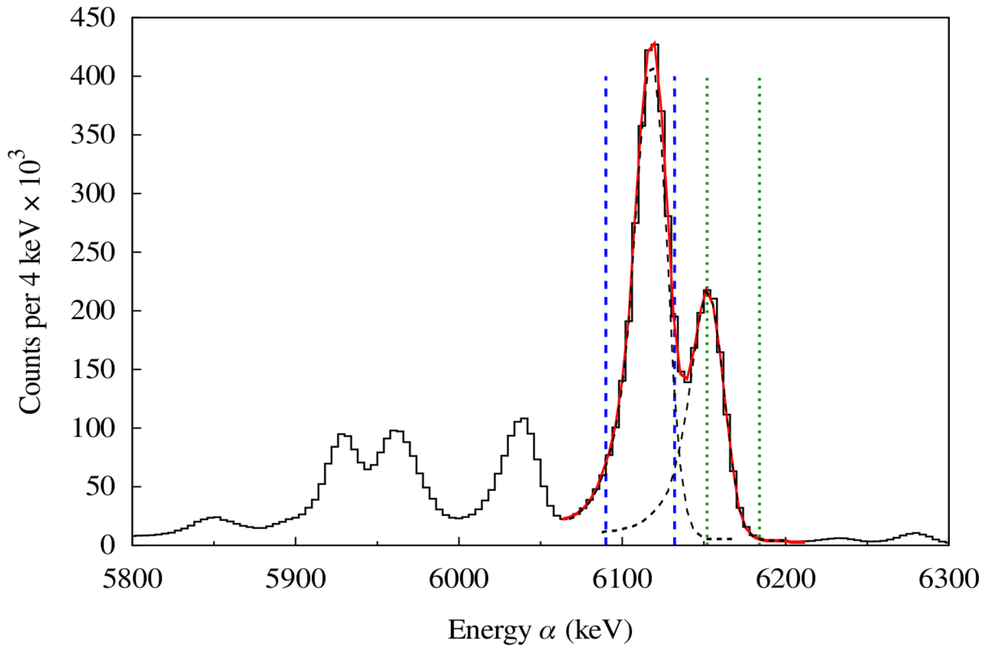

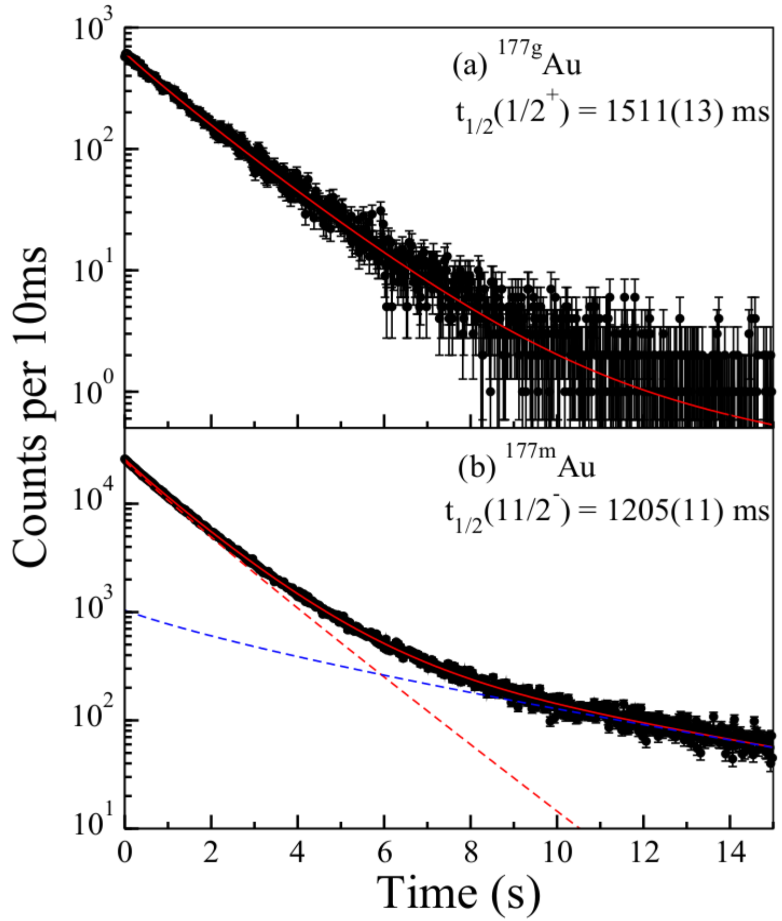

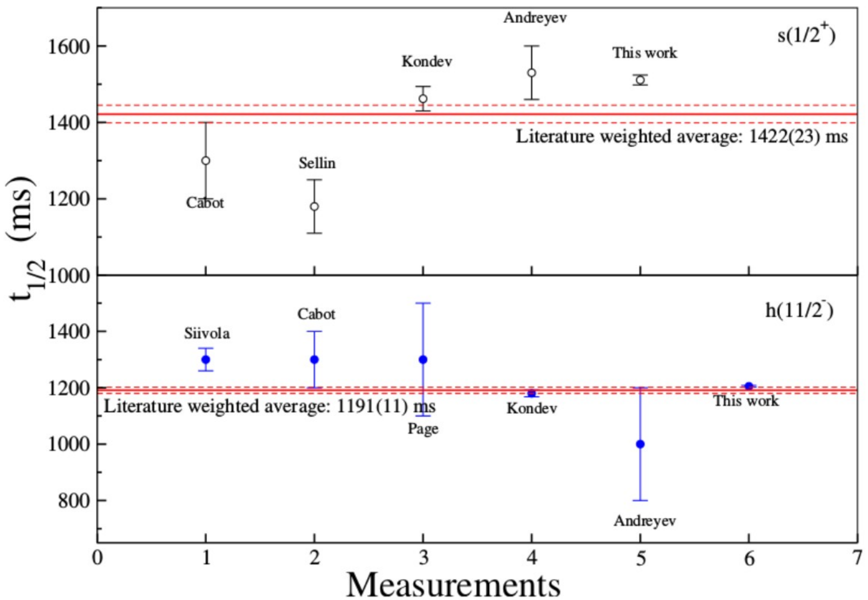

- Time difference between the the detection of gamma-biased recoil and its subsequent alpha-decay with in the same DSSD.
- Fit * background correction (to allow multiple implantation)
- Eliminate overlap by careful selection of alpha particle energy.

Deduced level scheme:

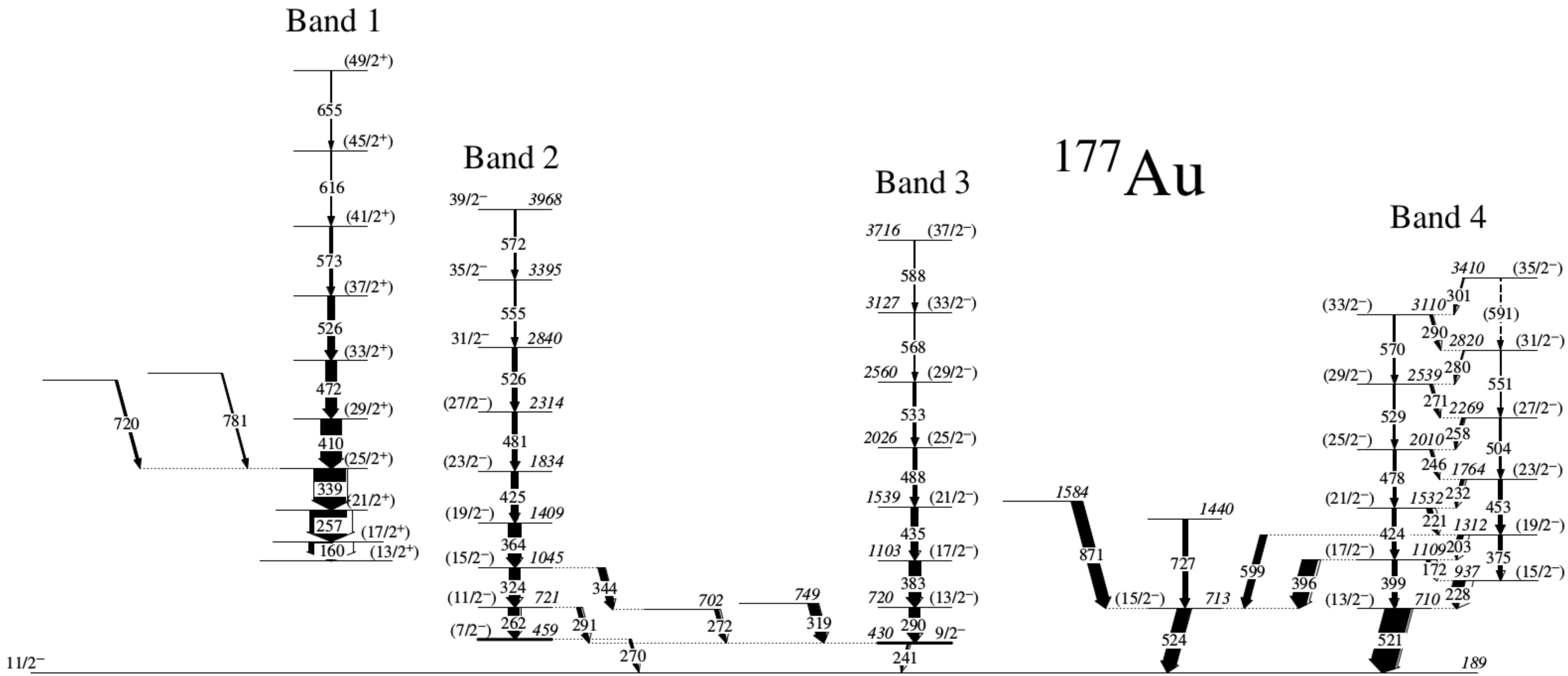

F. A. Ali at al. In preparation

Accepted for publication:
M. Venhart, F. A. Ali at al. Phys Rev. **C**

- Matrices tagged on the α decays from the 1/2 + and 11/2 − states contained a total of 2.0 × 10^5 and 6.3 × 10^ 5 α (^{177}Au)-tagged γ − γ events, respectively.

Assignment of Band 1

Band 1 - The $i_{13/2}$ intruder band:

- Band head had decay paths to both α decaying states are reordered.
- The first excited state is fixed to be 3/2+ at an excitation energy of 25(1) keV.
- consistent with A. Andreyev et al and M. Venhart et al. but with a greater precision.
- No discrete linking transitions connect the 13/2 + state.

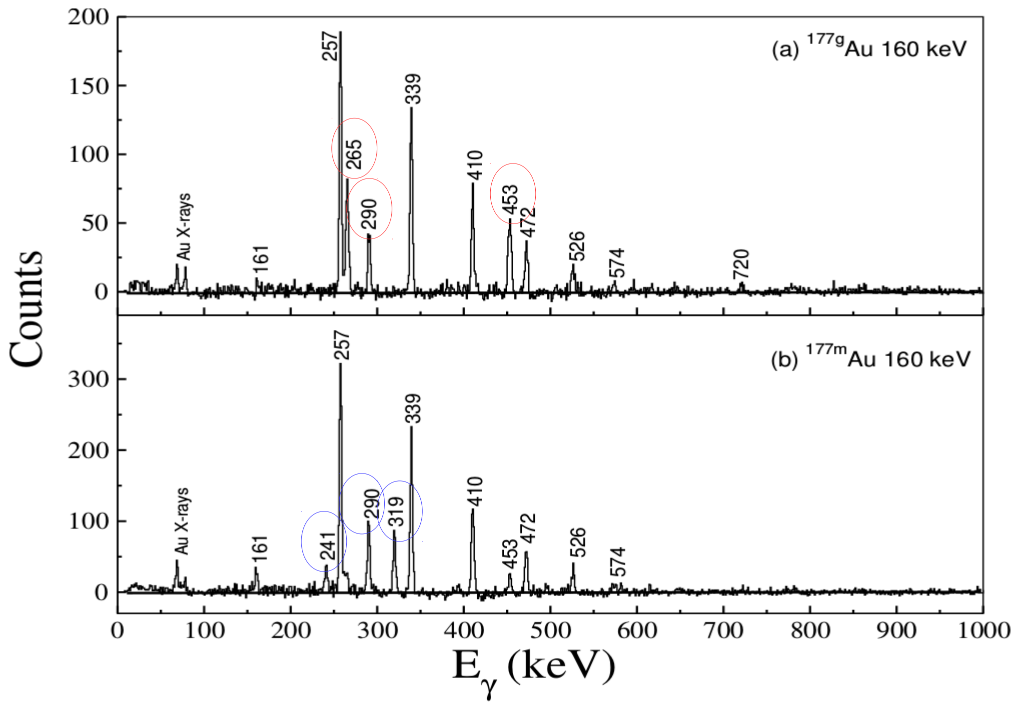

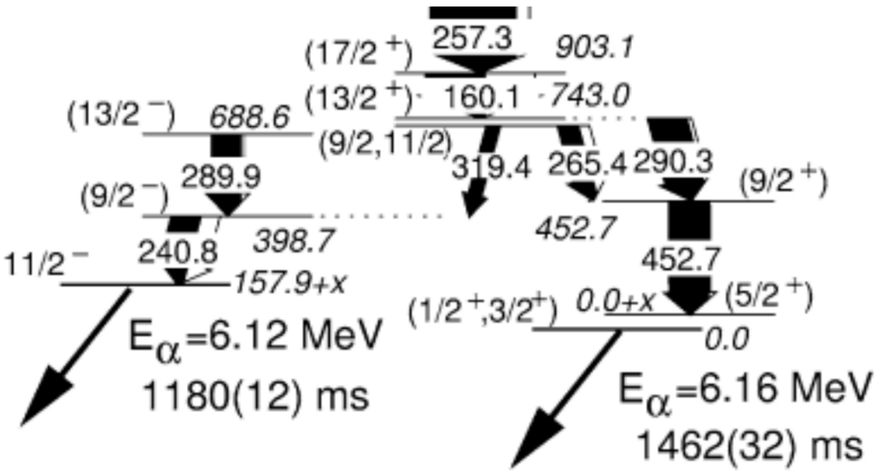

F. G. Kondev et al.

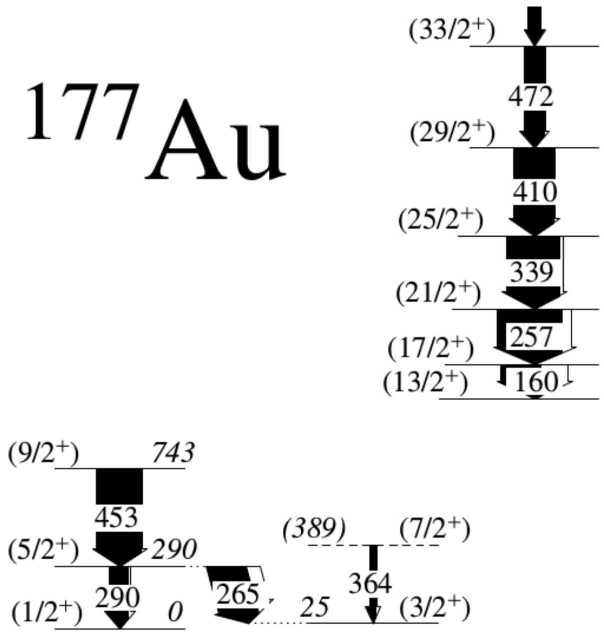

Band 1 - The $i_{13/2}$ intruder band:

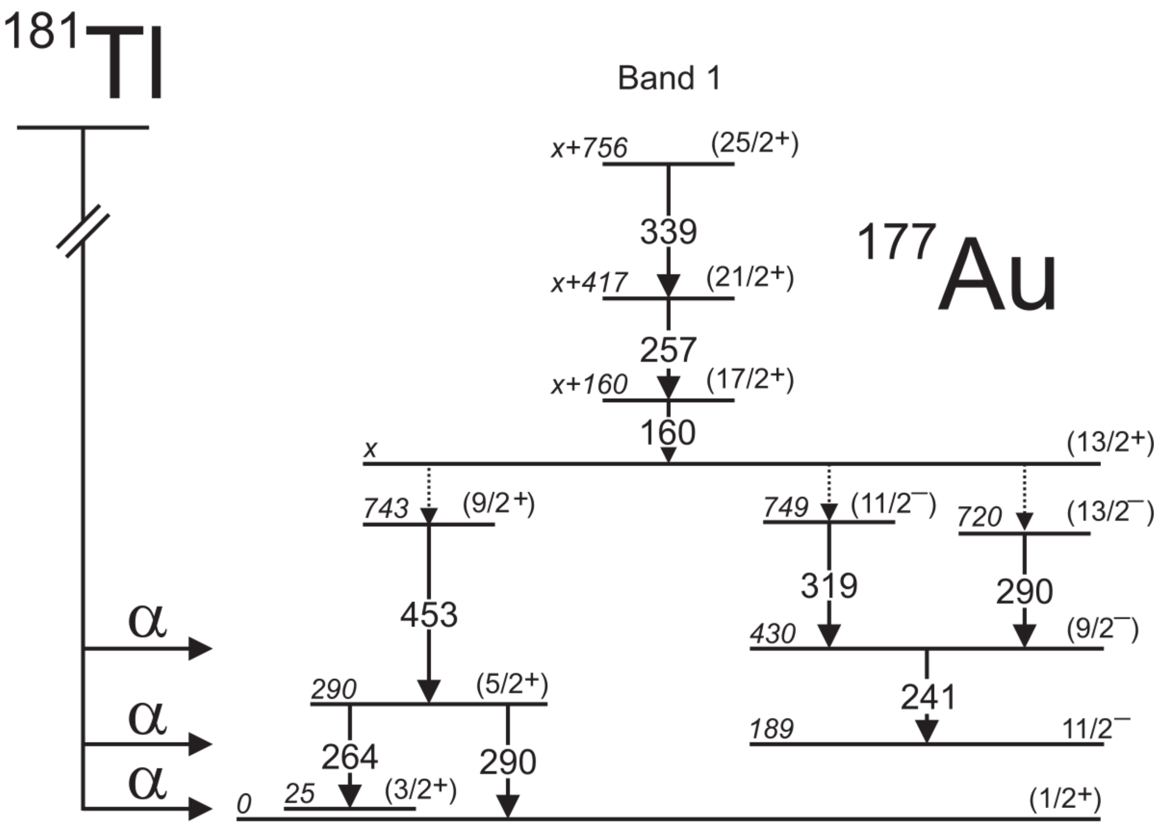

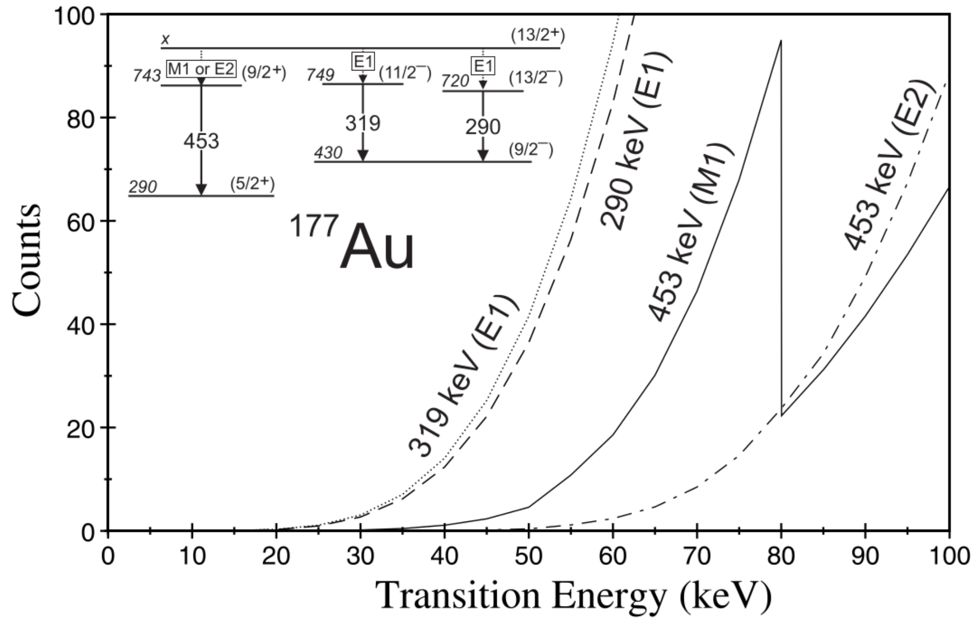

$$N_{counts} = \frac{I_{(T,d)}\eta_f}{1+\alpha_f}$$

- constrain the 13/2 + excitation energy to be no more than 40 keV above the 749 keV (11/2 −) level.
- dominance of the internal conversion process for low-energy transitions in this heavy nucleus.

The systematic trend in $i_{13/2}$:

- A parabolic dependence on the neutron number.
- A lower deformation resulting in a higher excitation energy of the $i_{13/2}$ intruder configuration.
- Thus it is likely that the $i_{13/2}$ intruder parabola reaches a minimum at N = 98.

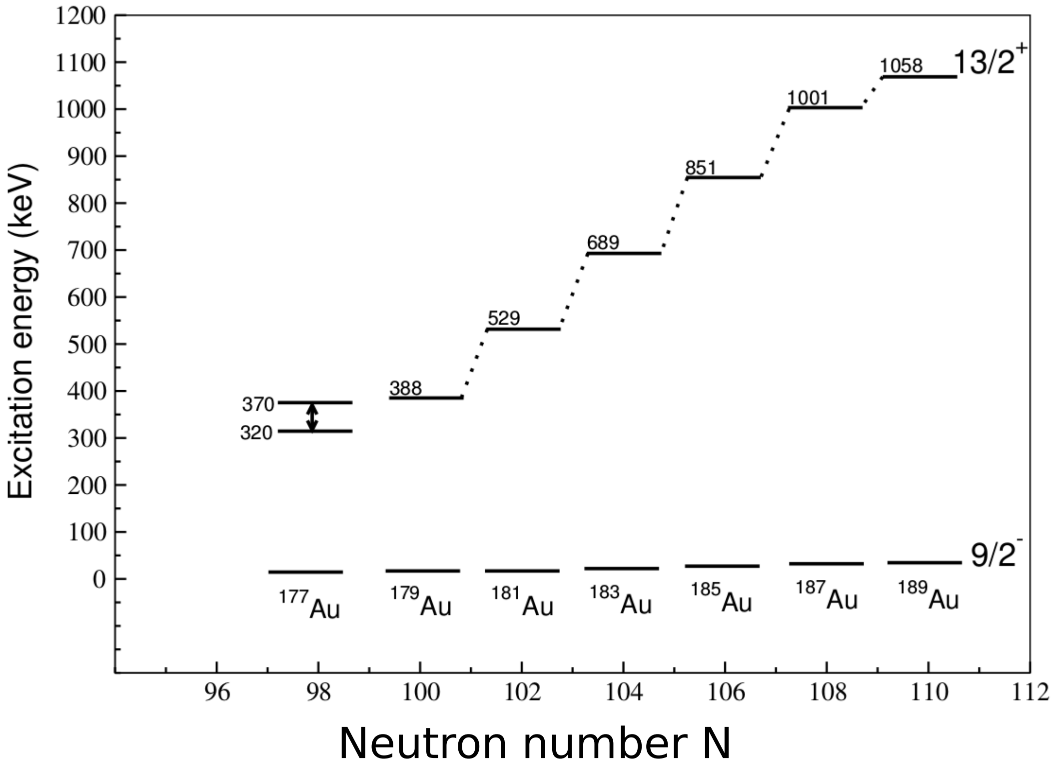

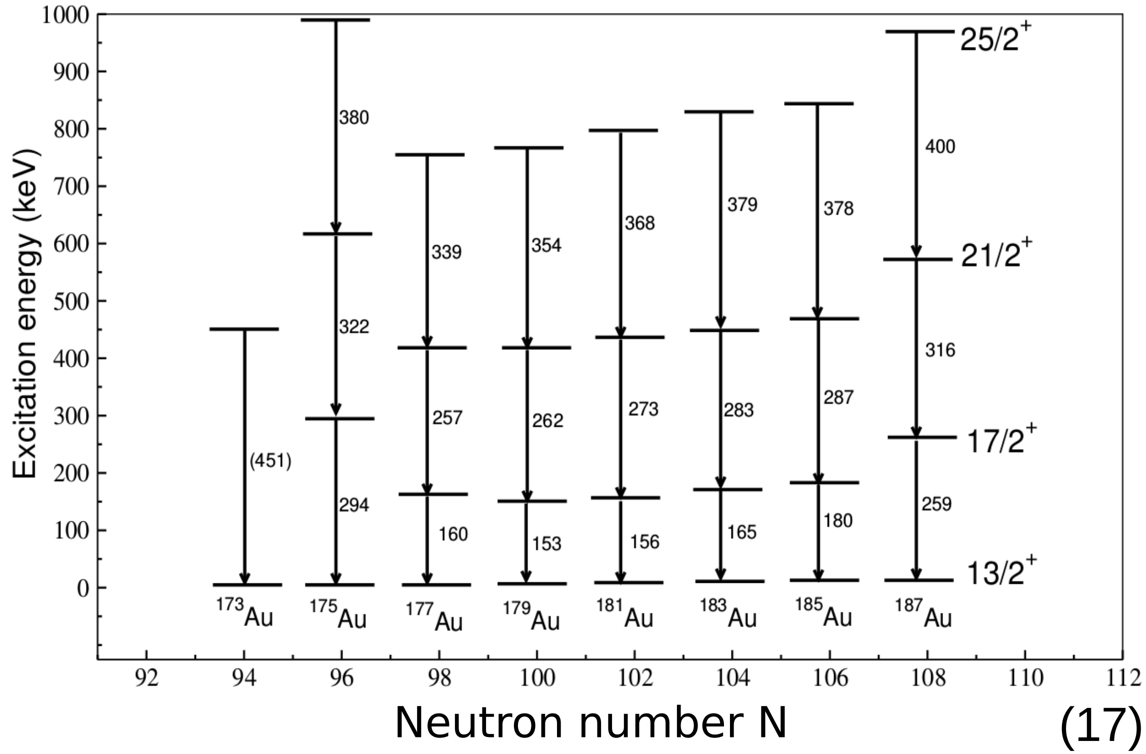

Assignment of Band 2 & Band 3

Band 2 - The $f_{7/2}$ intruder band:

- 3 decay path to decay paths to the 11/2 − isomer and no discrete transition decay path to ground state.
- Intensity of 271 keV compare to 262 keV, a short lived nano second isomer.
- Decay to the ground state is not fully identified although a 364 keV transition.
- 364 keV transition places some constraints on the various scenarios.

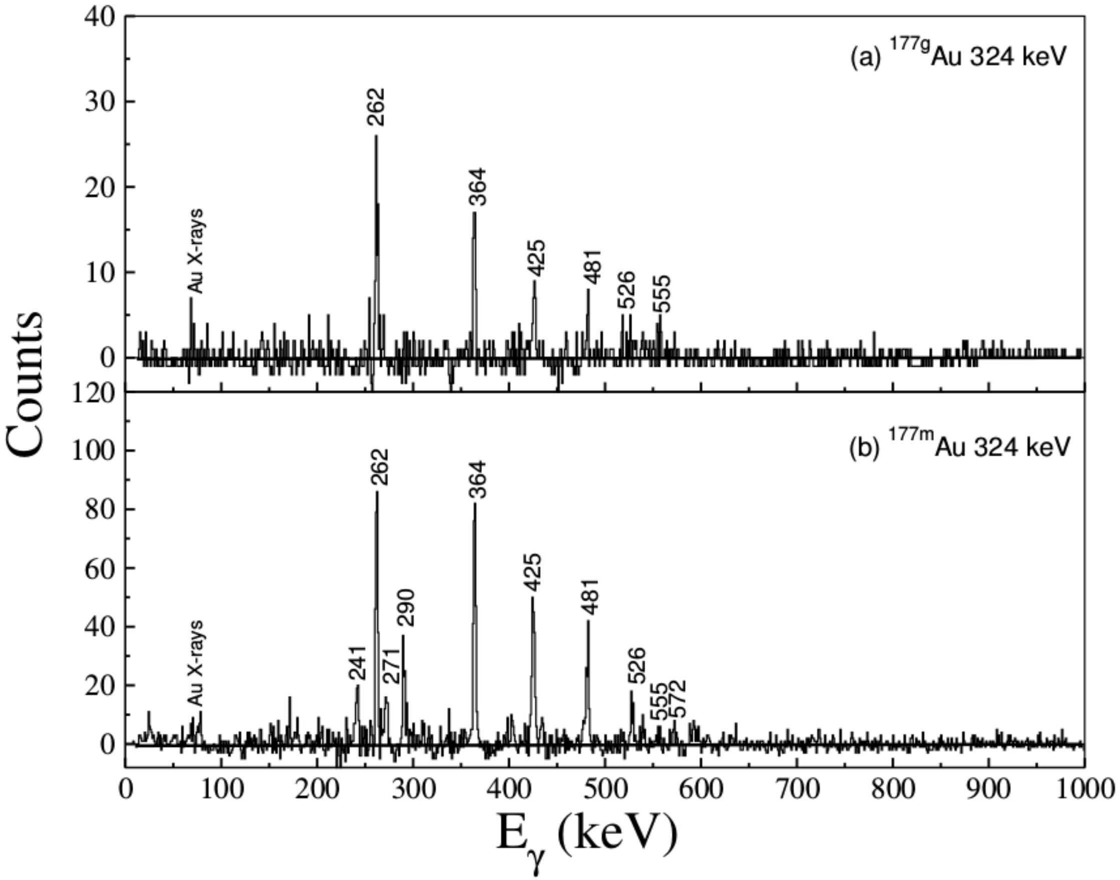

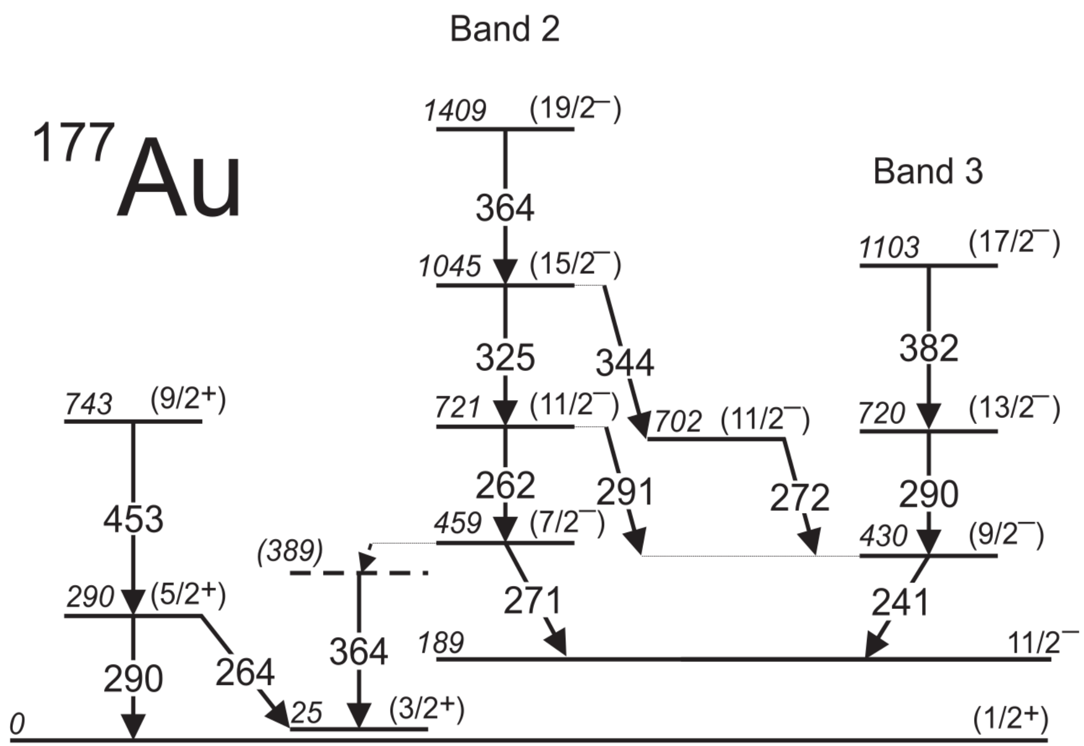

Band 3 - The $h_{9/2}$ intruder band:

- Included in the NNDC data tables, but there are no further details published in the literature.
- Decay paths to the negative-parity 11/2 − isomer via 241 keV exclusively.
- Intensity of 241 keV compare to 290 keV, a short lived nano-second isomer. Supported in a commissioning Experiment using SAGE γ-ray - conversion electron coincidence spectrometer. (IC. Electron)
- Anomalous conversion coefficient revealed for 9/2- state.

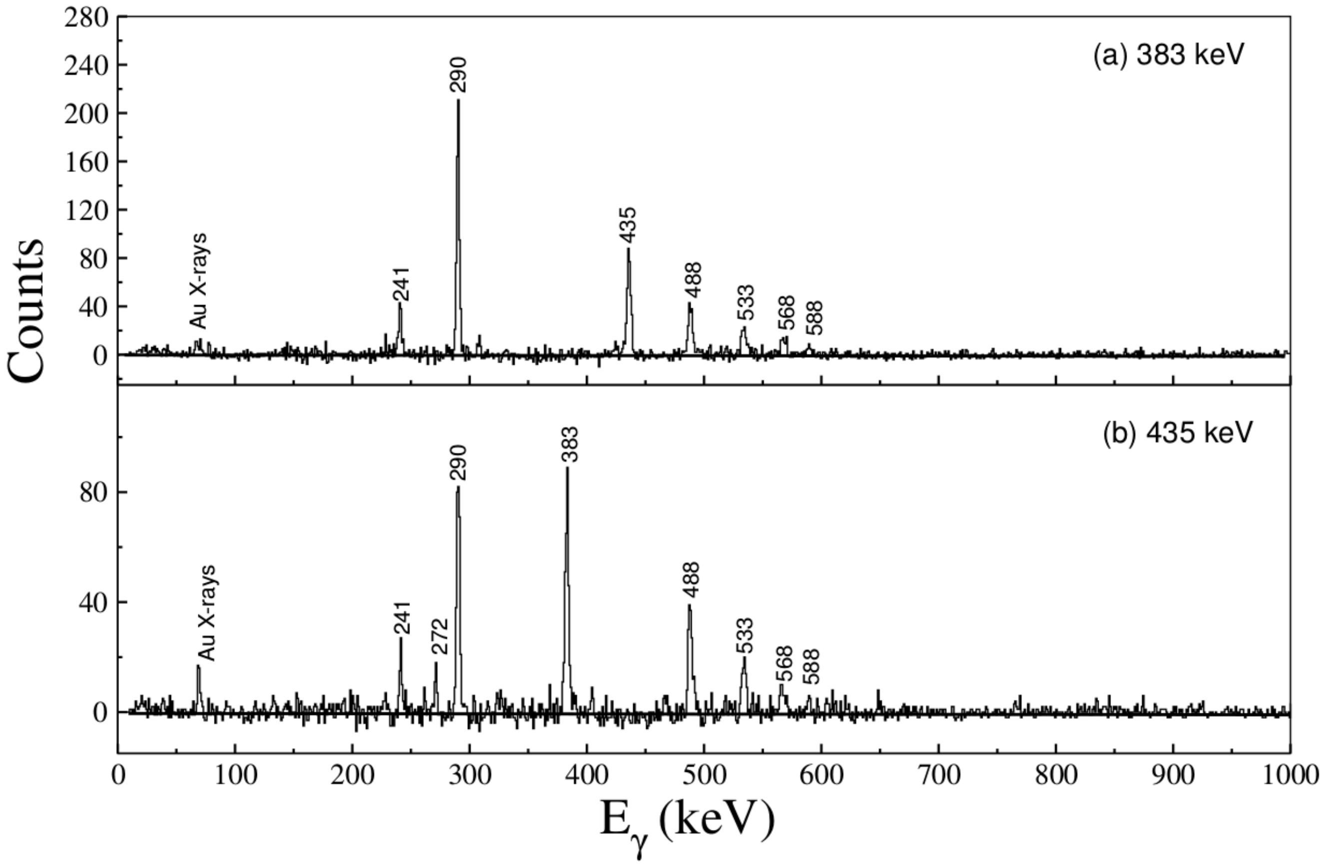

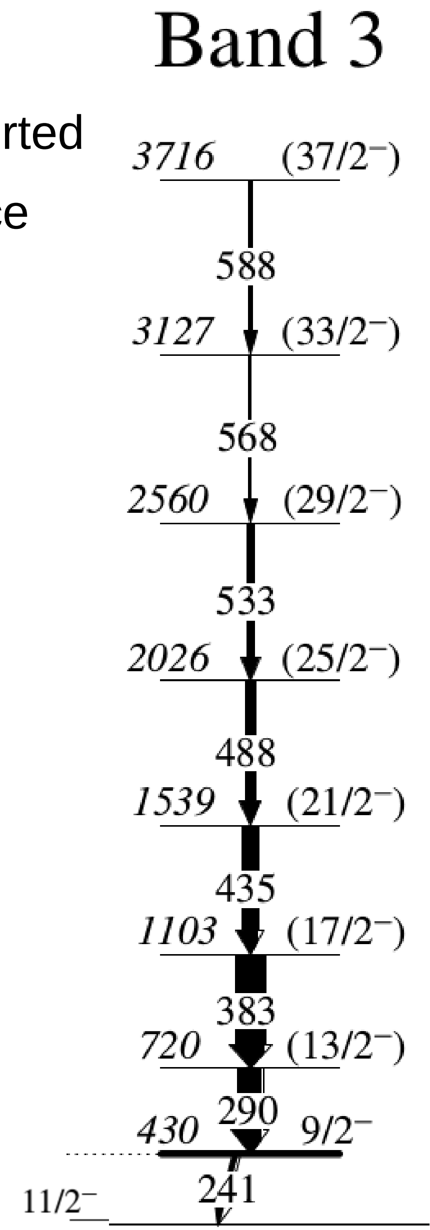

Systematic trends Band 2 and Band 3:

- Excitation energy 459 keV, Band 2, fit with a parabolic trend established for mixed $\pi(f_{7/2} \oplus h_{9/2})$ configuration.
- Passing the minimum at N=100.
- The trend reveals that the energy difference of the $\pi(f_{7/2})$ and $\pi(h_{9/2})$ single-particle states are closest in energy in ^{179}Au and the $\pi(h_{9/2})$ is always lower in excitation energy across the isotopic chain.
- Band 3, is assigned as the $\pi(h_{9/2})$ intruder configuration based on the 1/2−[541] Nilsson orbital. And to be a collective band with a prolate shape.

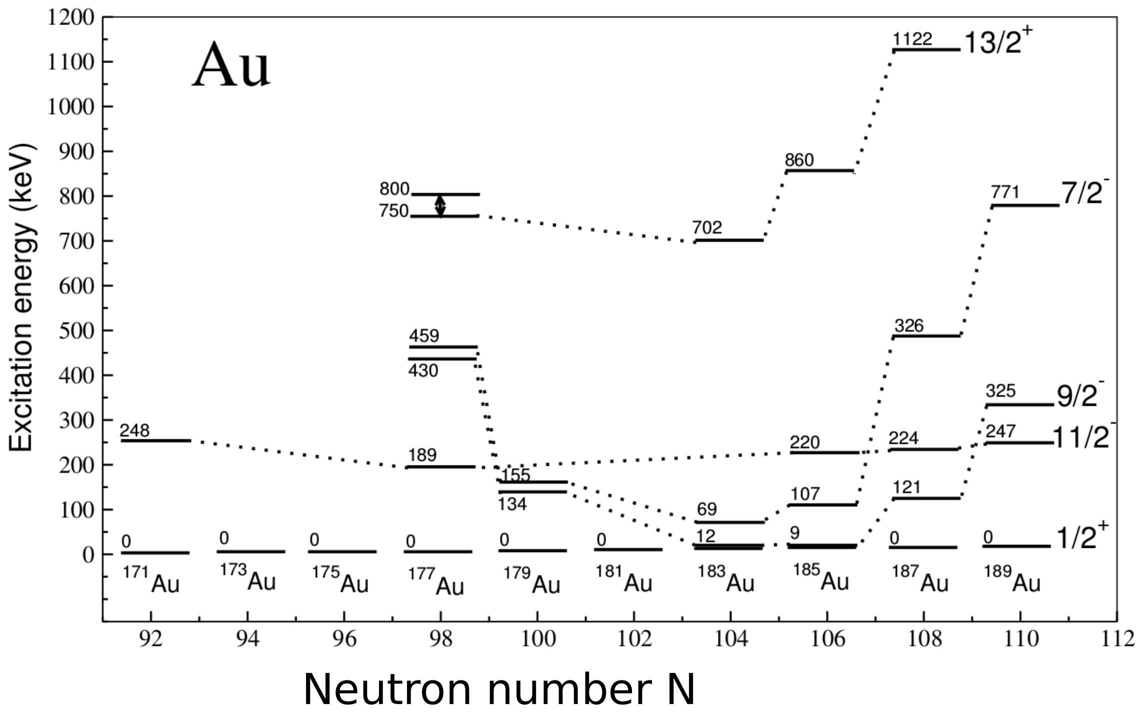

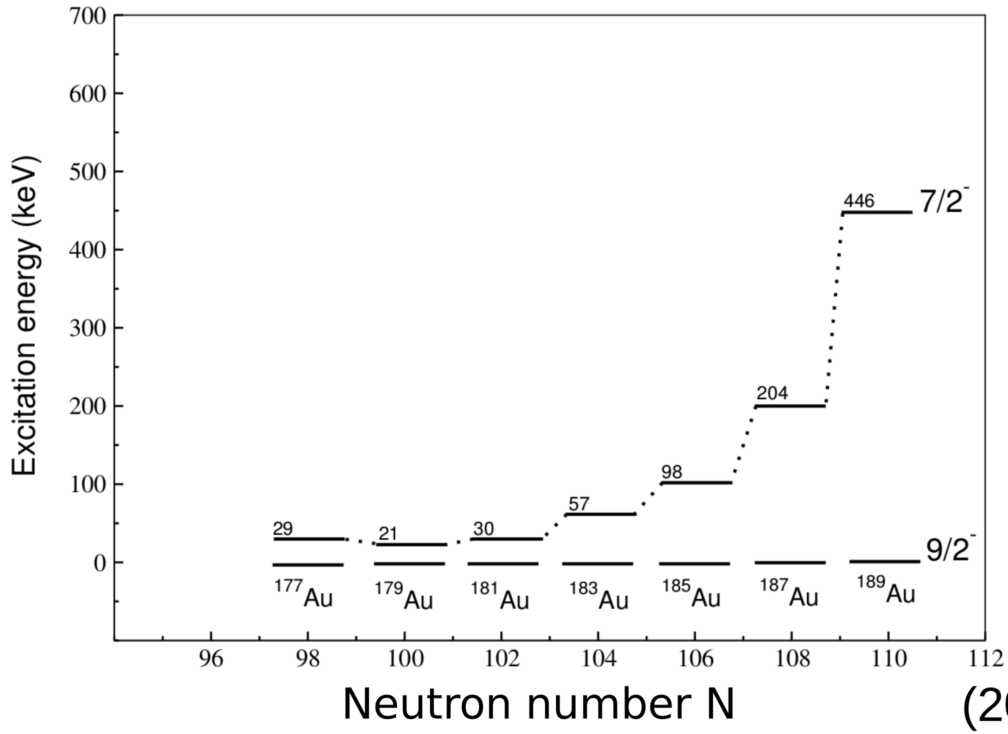

The kinematic moment of inertia:

- Information on the degree of deformation.
- Pb and Po to compare the bands in ^{177}Au.
- Bands can be considered as a proton or hole coupled to ^{176}Pt or ^{178}Hg cores.
- Both cores, have oblate ground states that are crossed by a prolate band at low spin. The core configurations are prolate at spins I > 6.
- prolate deformation of the the cores is predicted to be β 2 ~ 0.25 from potential energy surface calculations.
- Band 1 has a highest moment of inertia ->well deformed prolate shape.
- Band 2 & 3, are very similar to the moments of the cores. And consistent with prolate shape.

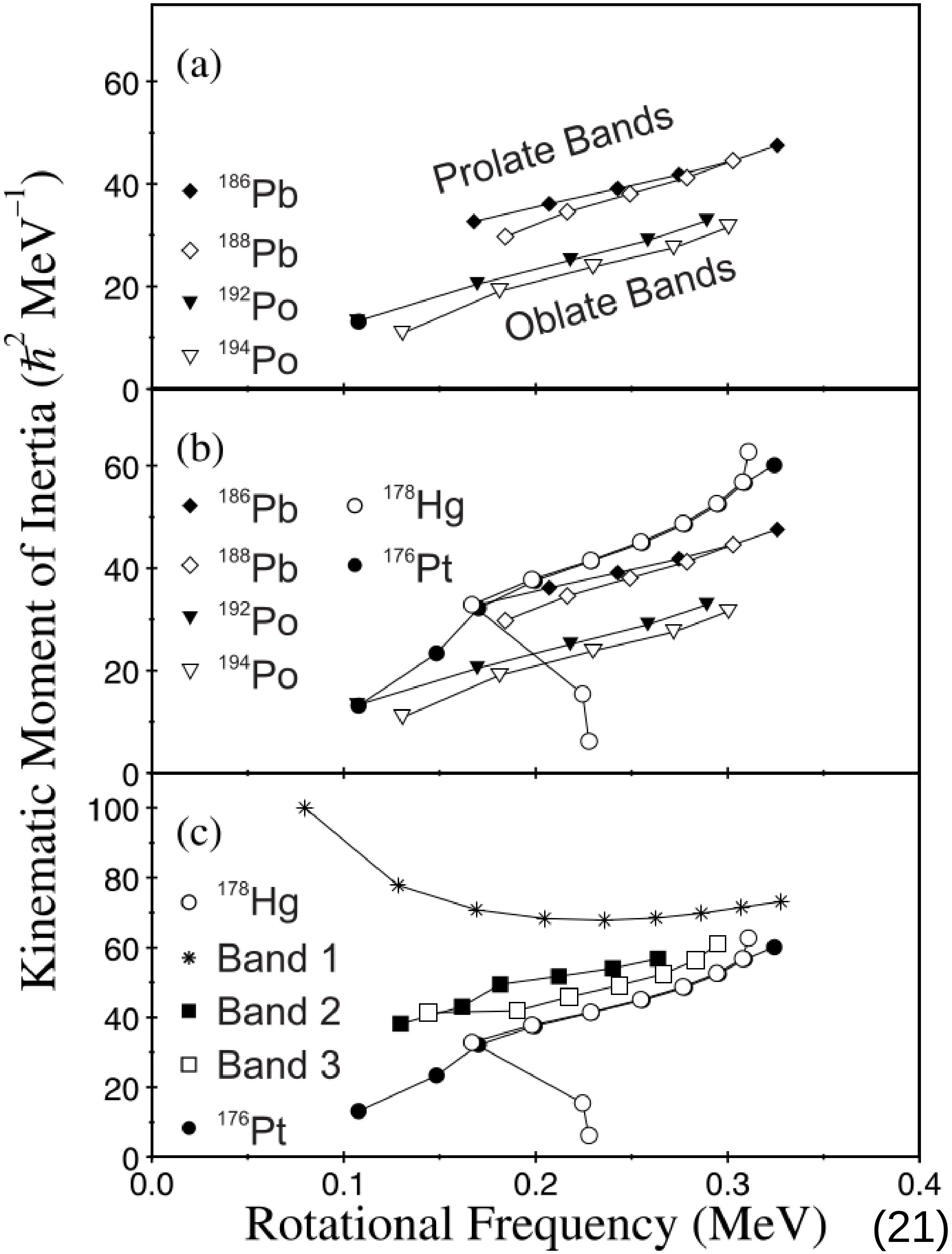

Band 4 Strongly Coupled Band (s.c.b.):

- Included in the NNDC. data tables, no further details published in the literature.
- 521keV transition that connects the lowest energy level observed in the strongly coupled band (Ex.=710keV) with the 11/2− α- emitting isomer.
- A state at an excitation energy 713keV, which decays directly to the 11/2− isomer through a 524keV γ ray.

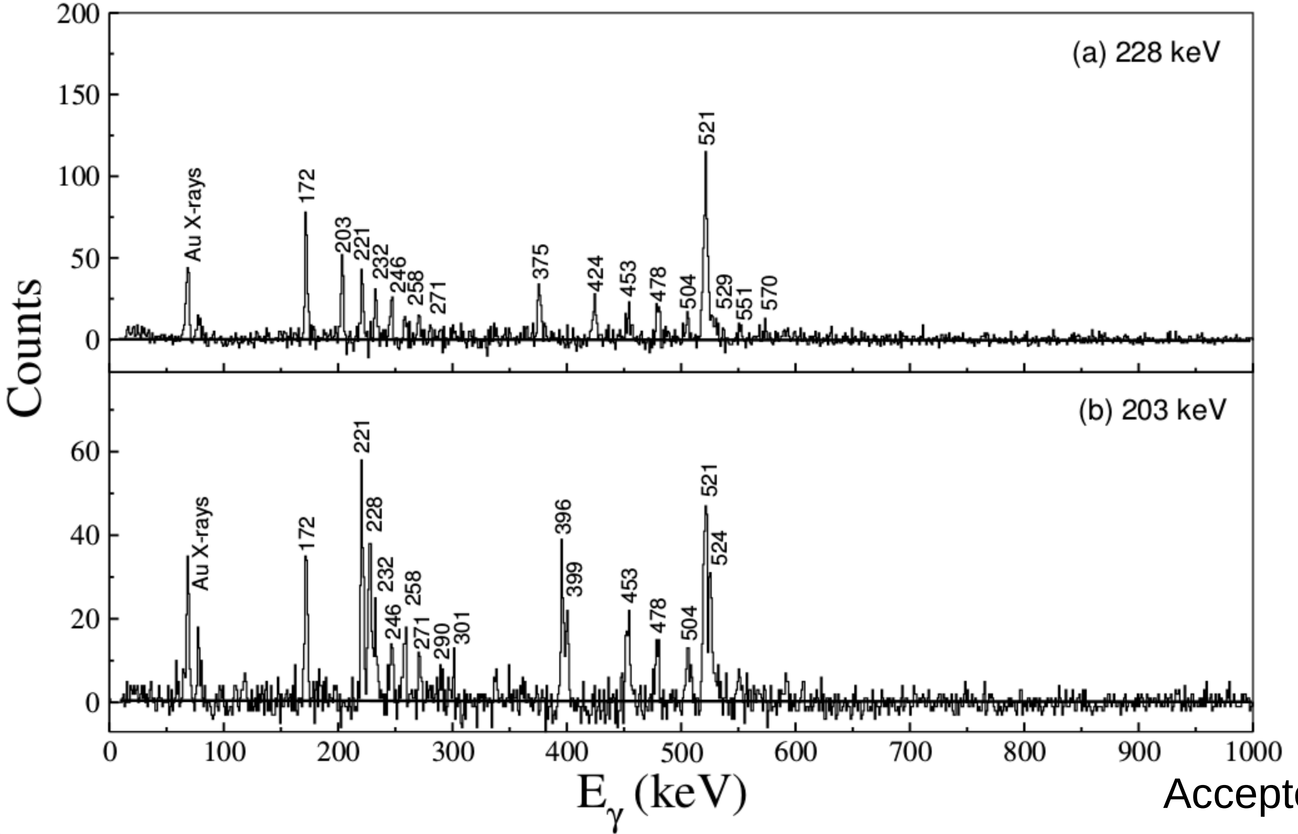

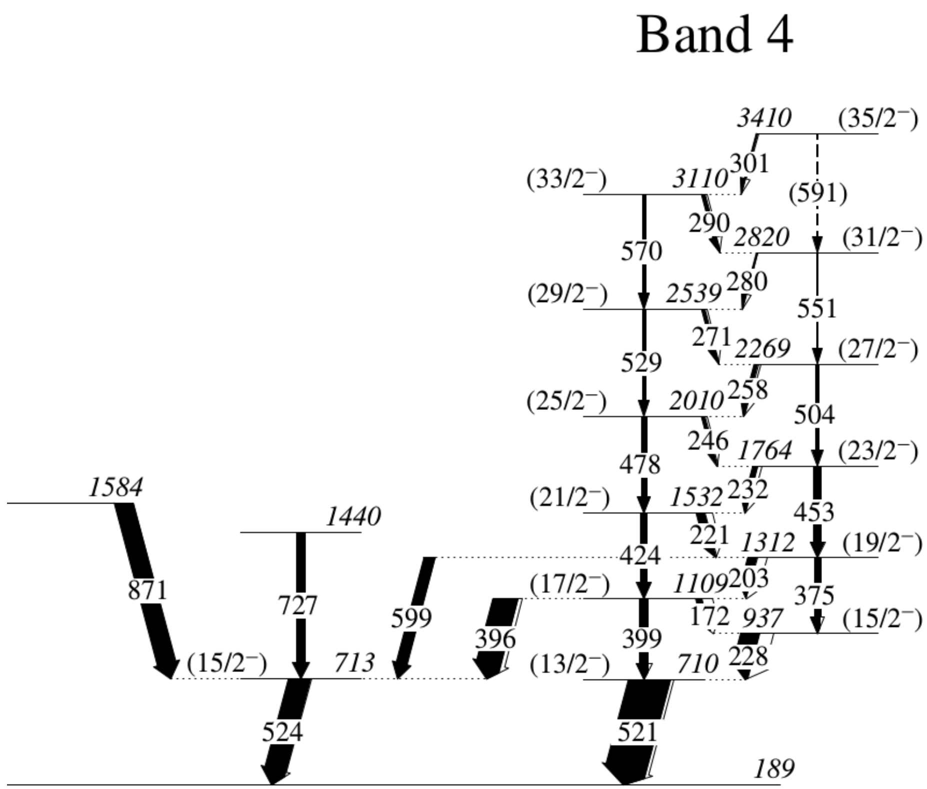

Accepted (M. Venhart, F. A. Ali at al. Phys Rev. **C**)

Band 4 Strongly Coupled Band (s.c.b.):

- Heavier Au isotopes -> either a few interconnected sates or the band appear as a floating band.
- A well developed s.c.b were firmly placed in the level scheme -> Unique observation in N- deficient -> probe shape coexistence and elucidate information on the underlying core.
- From both $B(M1{:}I \rightarrow I-1)/B(E2{:}I \rightarrow I-2)$ ratios and $\mathcal{J}^{(1)}$ Band 4 assigned to be a proton-hole configuration $(\pi h_{11/2})^{-1}$. and has a prolate shape respectively.
- The 11/2 − α- decaying isomer is interpreted as continuing the trend of a $\pi h_{11/2}$ hole coupled to the $^{A+1}$Hg core. Hg cores are oblate in their g.s. and at low spin. Thus the 11/2− isomer is likely to be an oblate configuration.
- Should also couple to the excitations of the ^{178}Hg core such as the **oblate** 2^+_1 state and the 0^+_2 **prolate** intruder state.

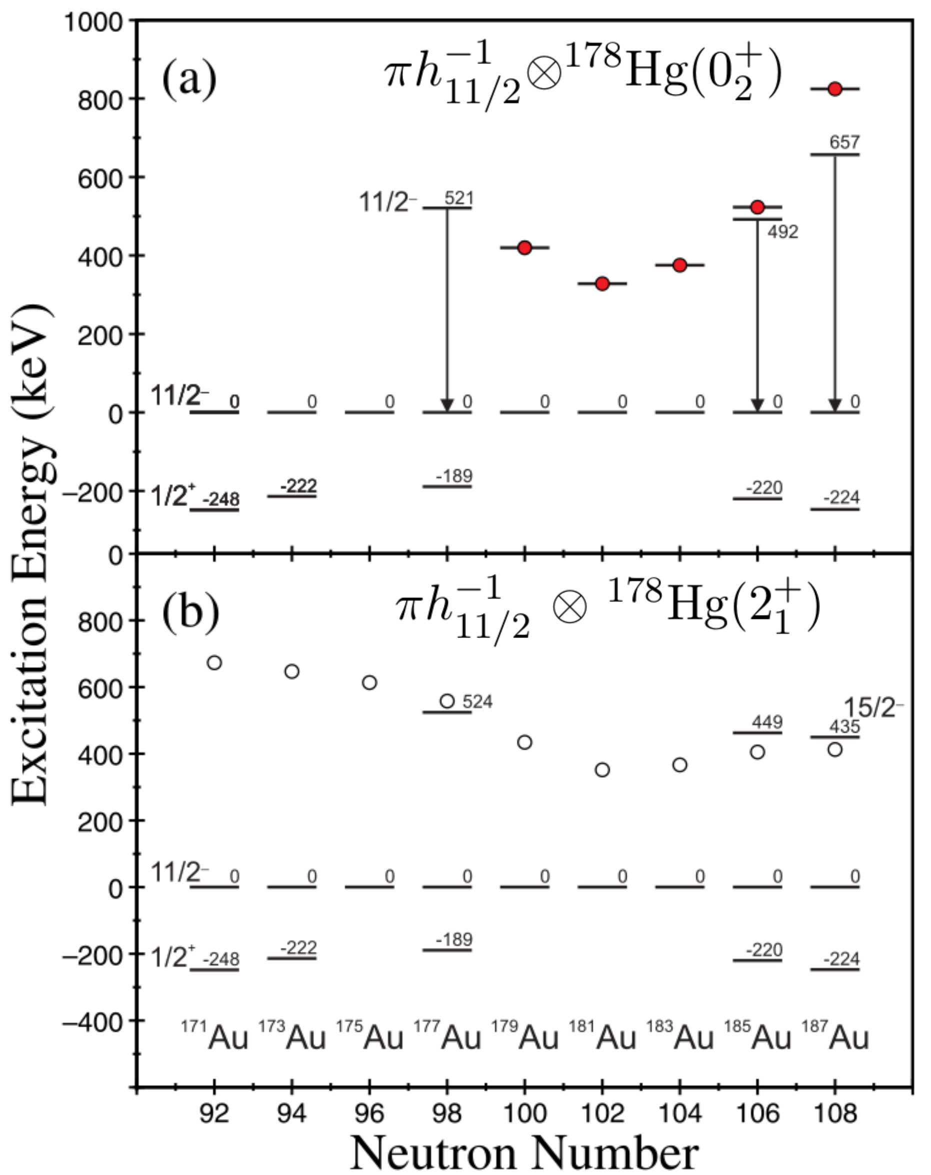

Conclusions:

- Gamma-ray spectroscopy using RDT experiment at JYFL allowed us to extract information on the single particle structure of ^{177}Au.
- A precise measurement of the half-life and Energy of the alpha- decaying states in ^{177}Au were achieved.
- The level scheme is extended greatly and the relative energy of nuclear states (and the shape associated with them) were determined.
- Two Nano-second ismoreic states are observed based on the intensity balance in this work.
- Excited states formed by coupling the odd $\pi h^{-1}_{11/2}$ proton hole to excitations of the ^{178}Hg core have been identified.
- Further studies of this type may provide evidence of the attribution of the intruder states (e.g. Tl) and improve our understanding of nuclear shape coexistence.
- Provides some encouragement for future experiments aimed at identifying new structures in other odd-Z nuclei near the proton drip line.

Collaborators:

Thanks to my Collaborators and you for listening ...

D.T. Joss, R.D. Page , R.D. Rolf-D. Herzberg, R.J. Carroll, C. McPeake, D. O'Donnell, B. Saygi, A. Thornthwaite.

Oliver Lodge Laboratory, University of Liverpool, Liverpool, L69 7ZE, UK.

M. Venhart, D. Klc, V. Matousek, M. Sedlak, M. Veselsky.

Institute of Physics, Slovak Academy of Sciences, SK-84511 Bratislava, Slovakia.

K. Aurannen, T. Grahn, P. T. Greenlees, A. Herzan, U. Jakobsson, R. Julin, S. Juutinen, J. Konki, M. Leino, J. Pakarinen, J. Partanen, P. Peura, P. Rahikila, P. Ruotsalainen, J. Saren, M. Sandzelius, C. Scholey, J. Sorri, S. Stolze, A. J. Uusitalo.

Department of Physics, University of Jyväskylä, FIN-40014 Jyväskylä, Finland.

J. L. Easton, E. Lawrie.

iThemba Laboratory for Accelerator Based Sciences, PO Box 722, Somerset West 7129 South Africa.

A. Andreyev.

Physics Department, University of York, Heslington, York, YO10 5DD,UK.

J. Simpson

STFC Daresbury Laboratory, Daresbury, Warrington, WA4 4AD, UK.

HCDP programme.

Ministry of higher education in Kurdistan Region –Iraq.

$$(A_0 e^{-\lambda_A t} + c) f(t),$$

The function f (t) is deduced from the time difference between successive recoil implantations that are followed by an α particle within the same DSSD pixel and was obtained by fitting a sum of four exponential functions, which is normalized

$$f(t) = \sum_{i=1}^{4} a_i e^{-b_i t}$$

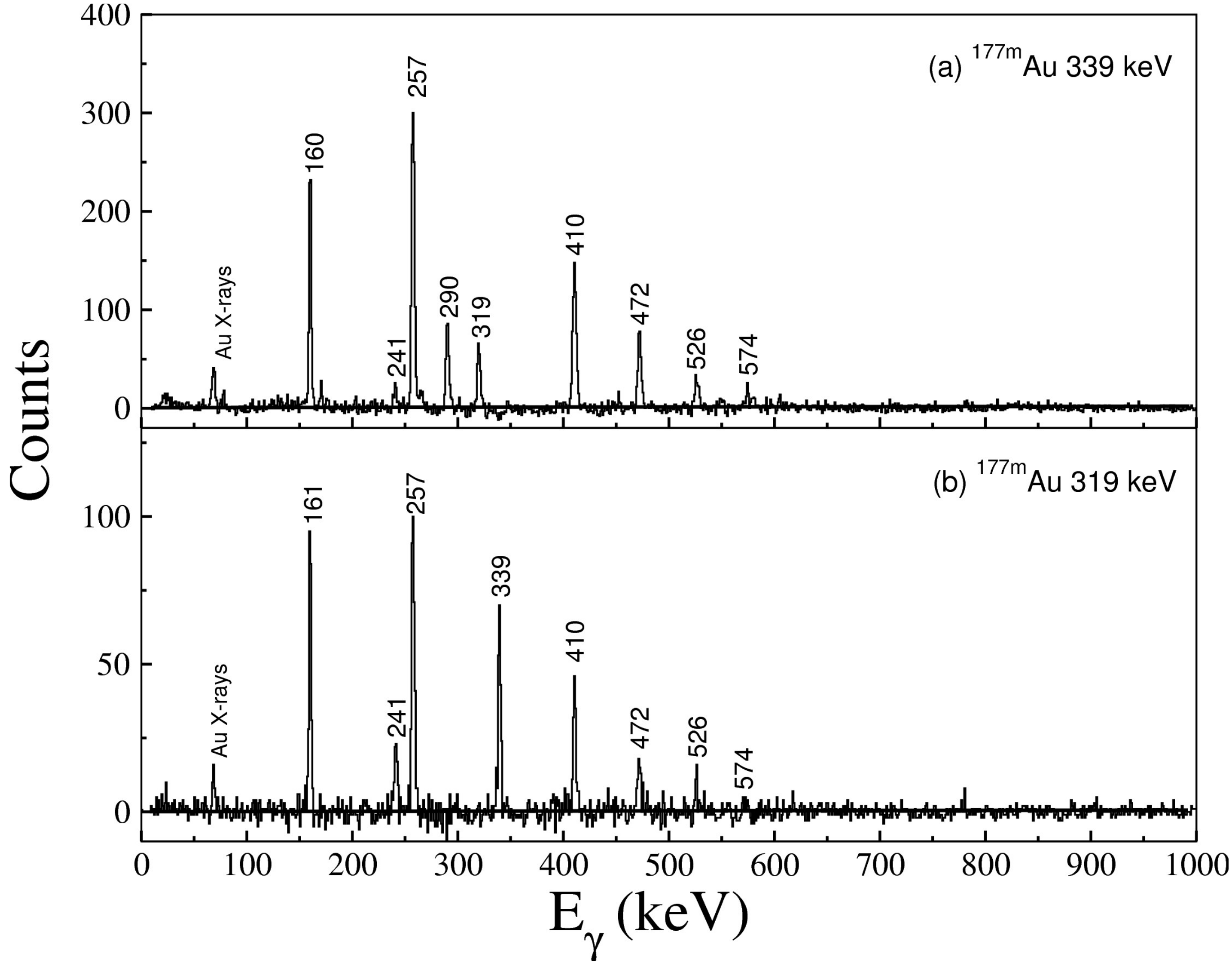

(a) 177mAu 339 keV
(b) 177mAu 319 keV
Counts
Eγ (keV)
Au X-rays
160
161
241
257
290
319
339
410
472
526
574
0
100
200
300
400
50
500
600
700
800
900
1000

Data Acquisition System (TDR):

- Eliminate the problem of common dead time from the composite detection system.
- signal is time stamped with reference to a system wide clock to a precision of 10ns. And constructed in the software rather than by conventional hardware triggering.
- event builder constructs the events for storage.

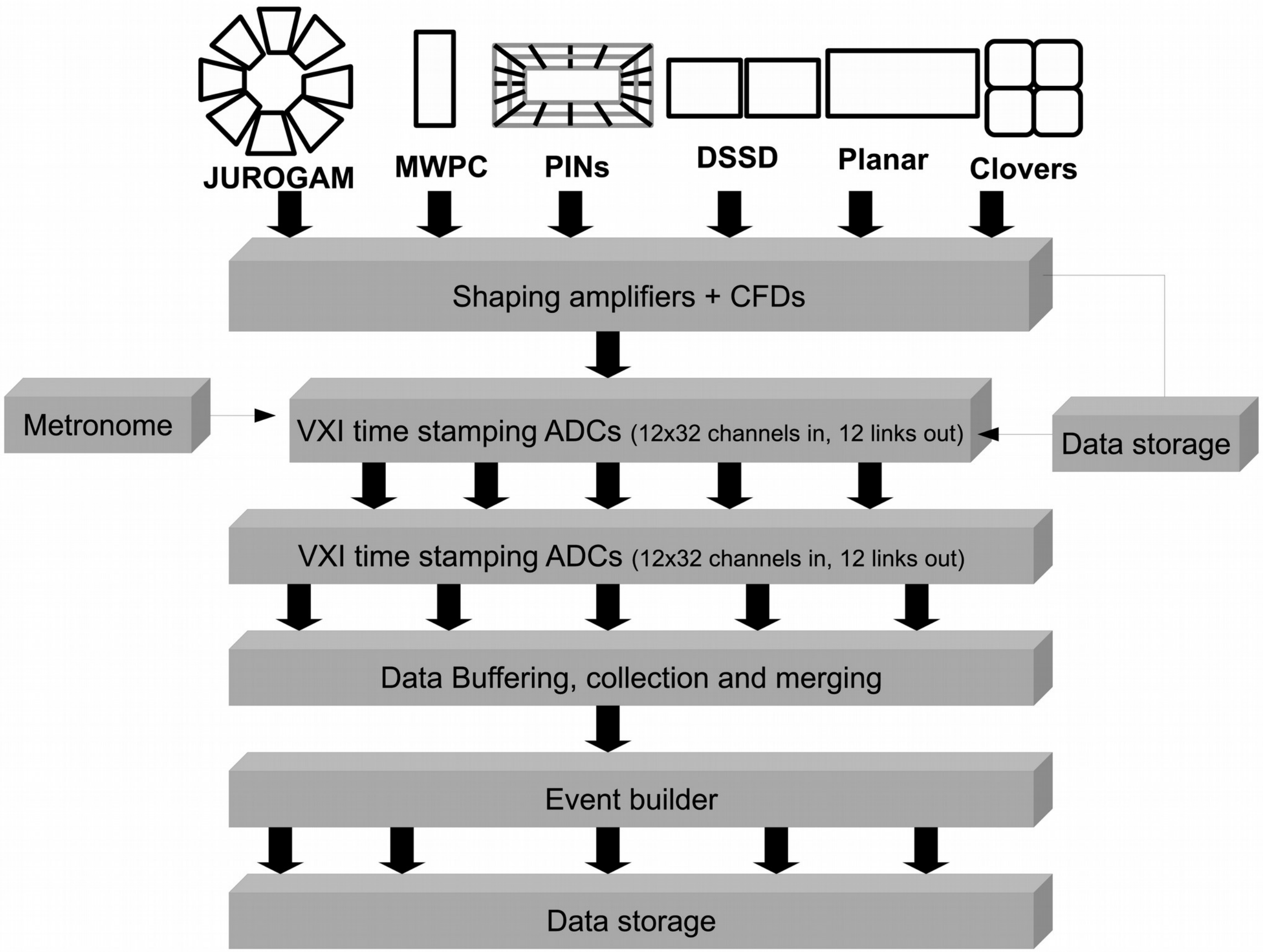

GRAIN software package used to analysis the data...

Recoil-alpha correlation in ^{177}Au:

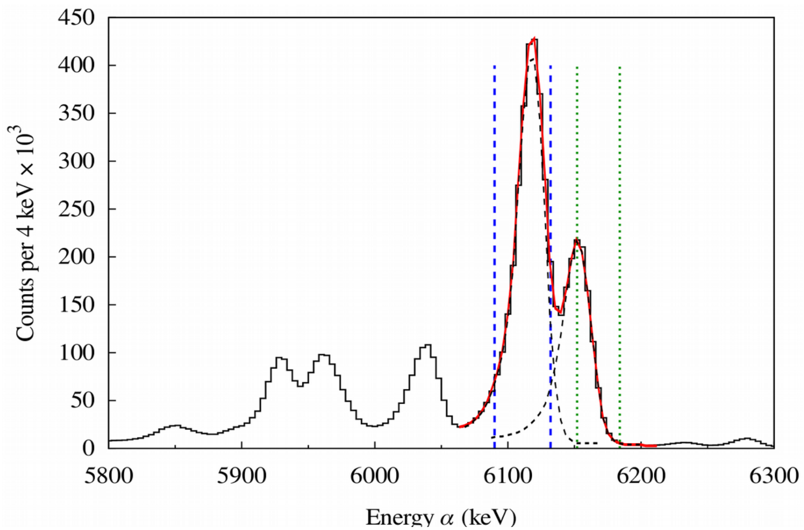

- Matrices tagged on the α decays from the 1/2 + and 11/2 − states contained a total of 2.0 × 10^5 and 6.3 × 10^ 5 α (^{177}Au)-tagged γ − γ events, respectively.
- Gamma-rays originating from other structure in ^{177}Au.

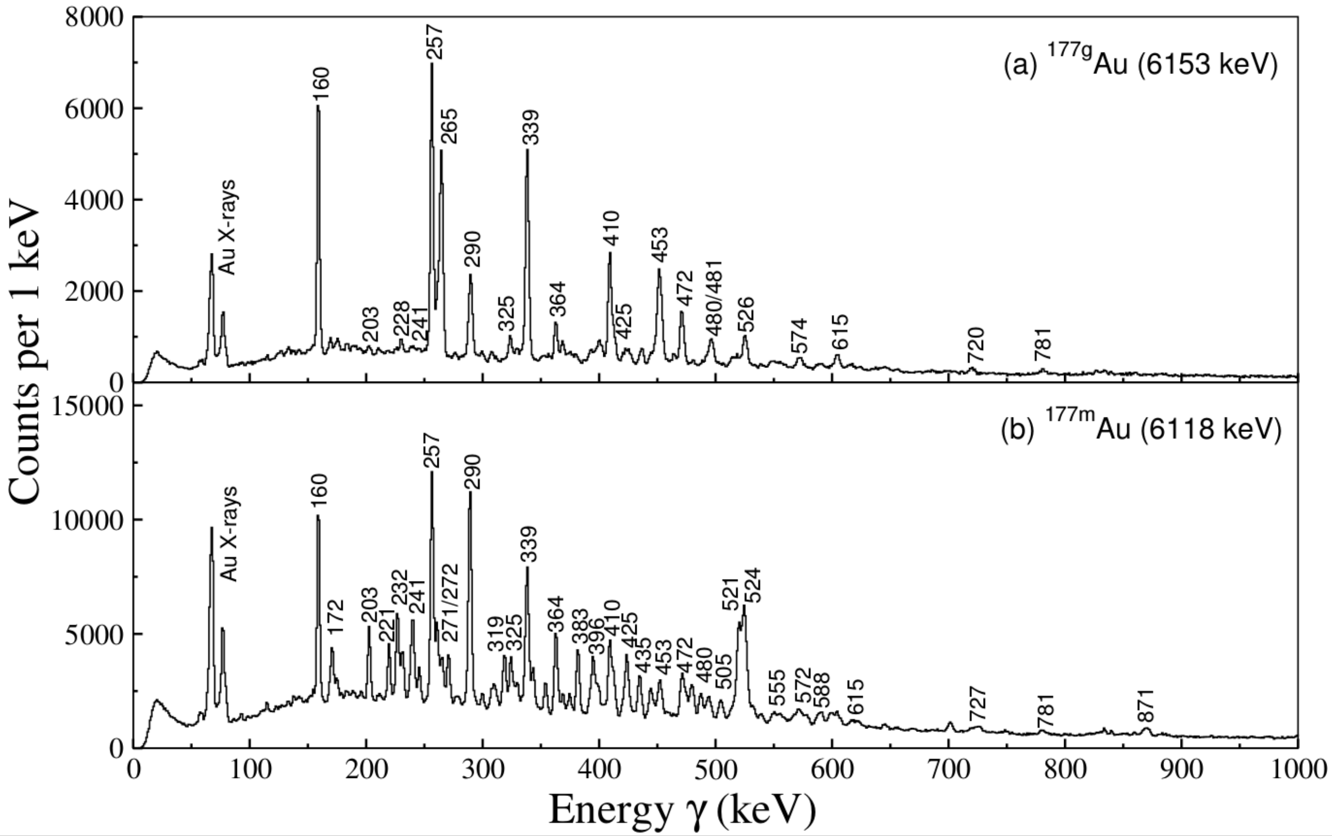

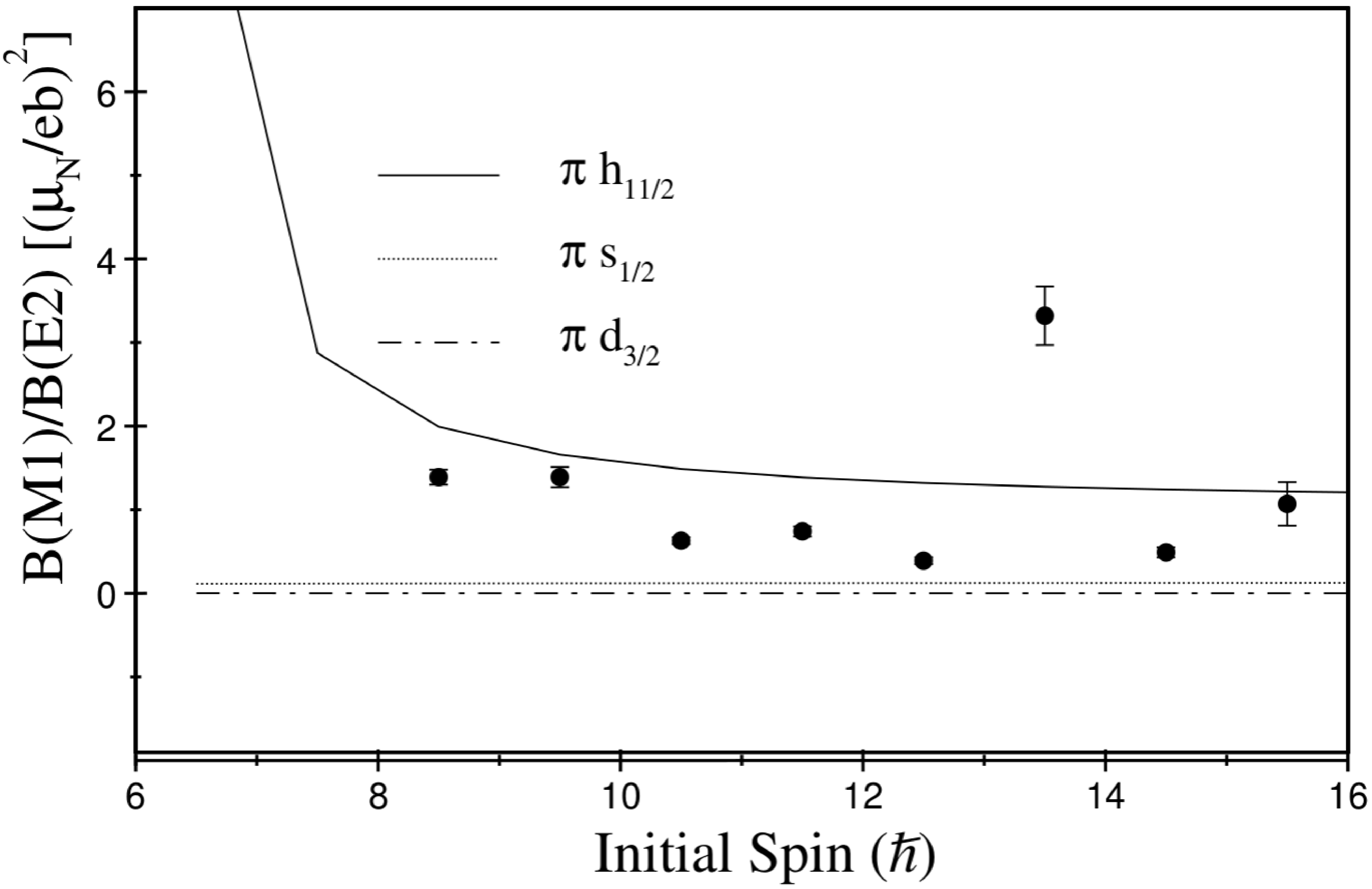

B(M1)/B(E2) [(μ_N/eb)^2]
6
4
2
0
π h_11/2
π s_1/2
π d_3/2
6
8
10
12
14
16
Initial Spin (ħ)

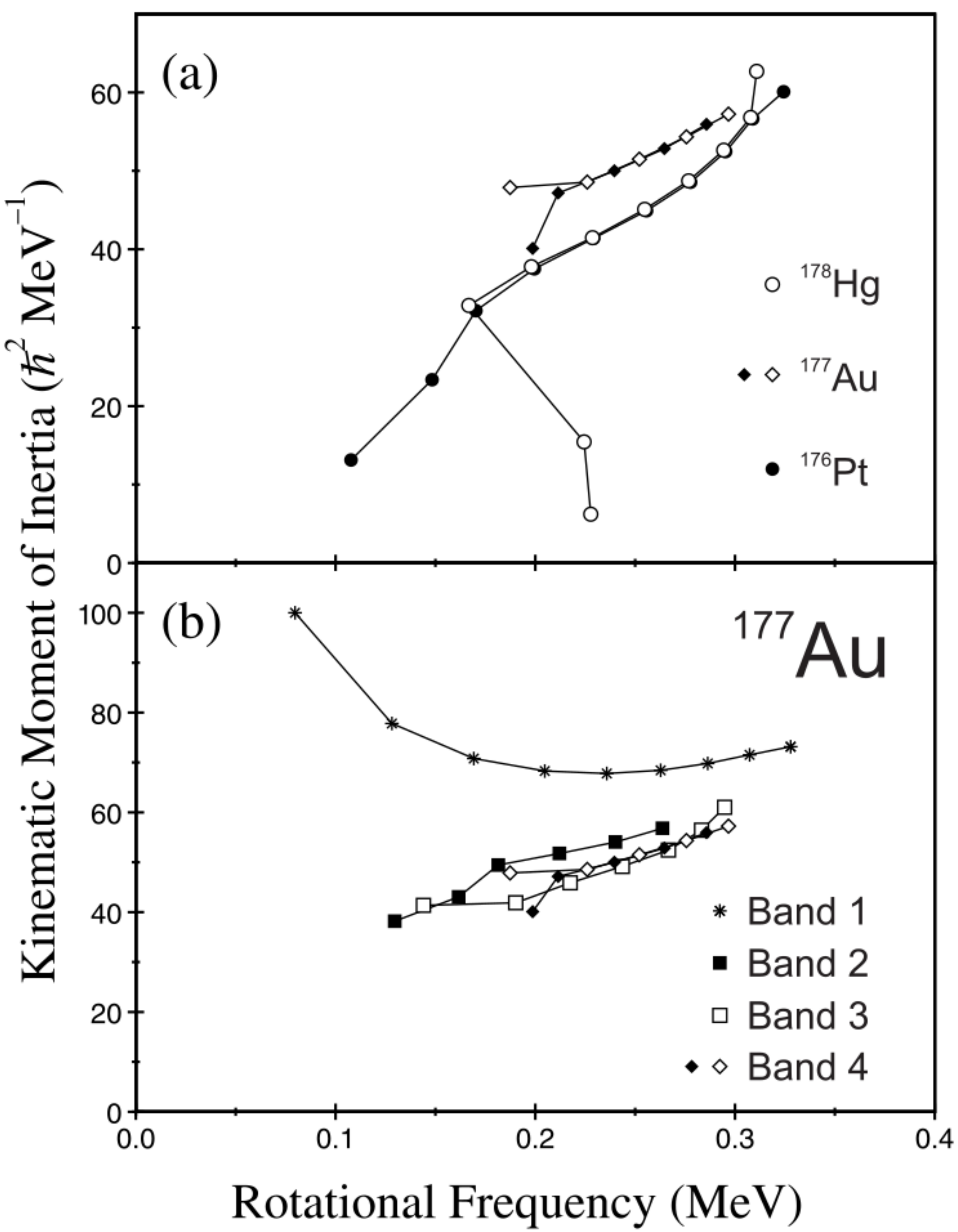

(a)
(b)
^{178}Hg
^{177}Au
^{176}Pt
^{177}Au
Band 1
Band 2
Band 3
Band 4
Kinematic Moment of Inertia ($\hbar^2$ MeV^{-1})
Rotational Frequency (MeV)
0
20
40
60
80
100
0.0
0.1
0.2
0.3
0.4

Band 1

- Decay paths from the $i_{13/2}$ intruder to the ground state have not been established completely across the range of isotopes.

Band 2 Band 3

- Absence of a decay path to g.s -> parity-changing transition of higher multipolarity from the 9/2 − band head is required, unlikely to be competitive.

Shape associated in the deduced level scheme:

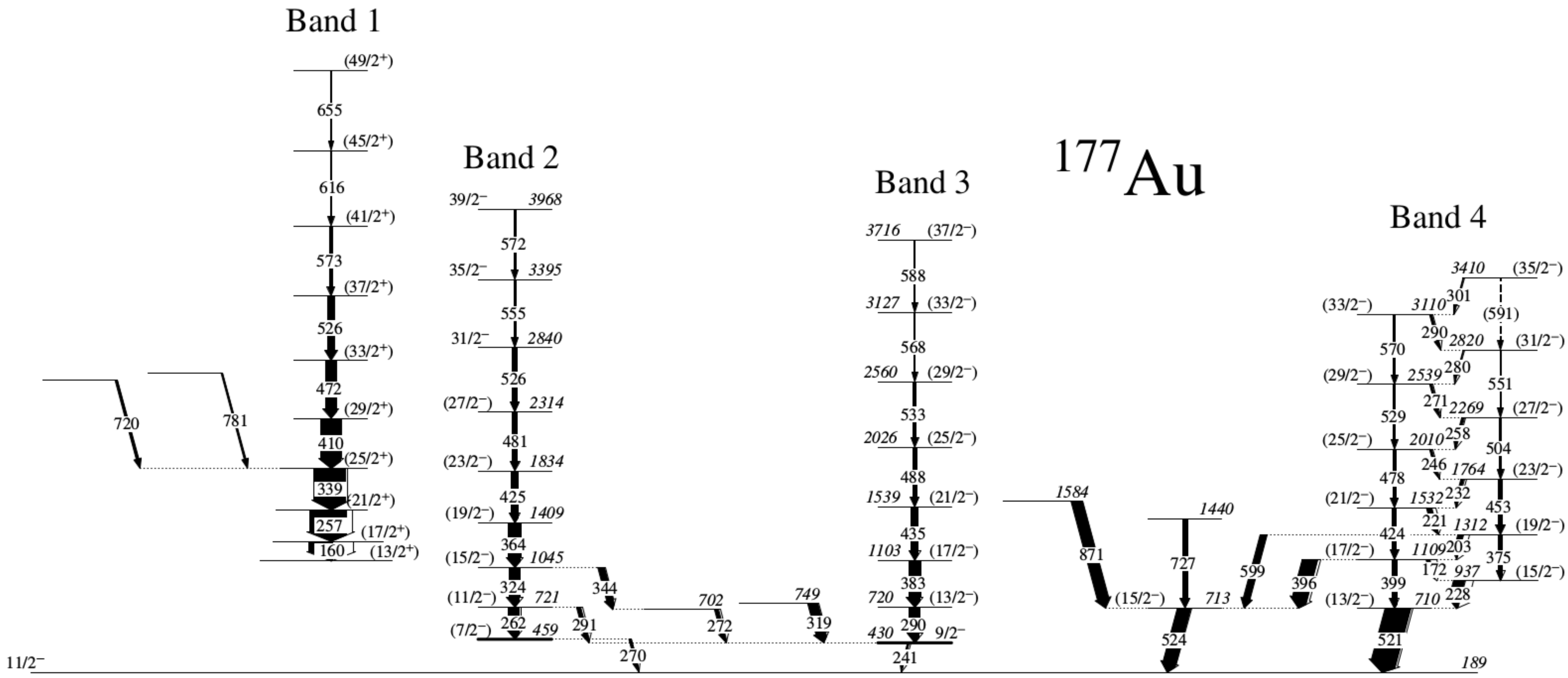

Prolate Prolate Prolate Oblate Prolate

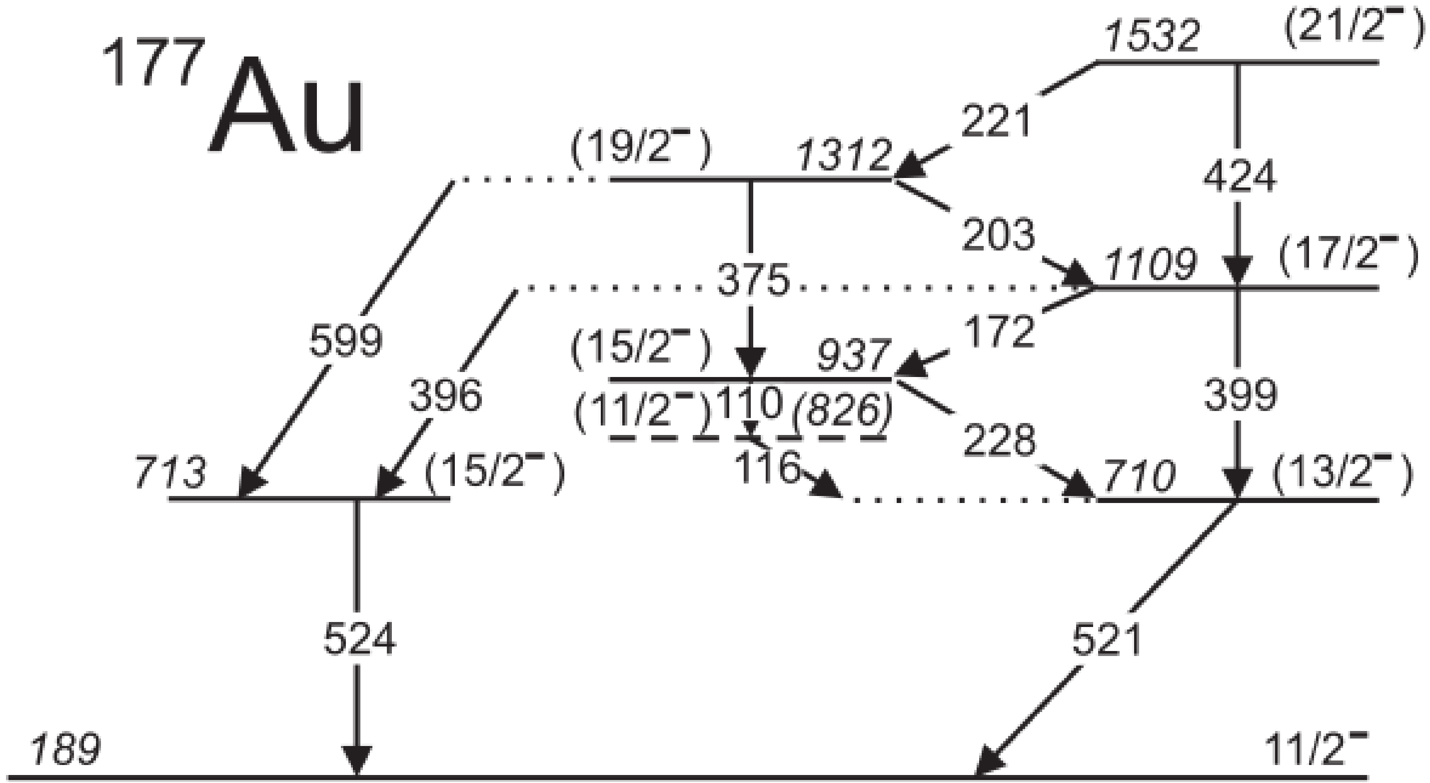

177Au
1532
(21/2−)
221
424
(19/2−)
1312
203
1109
(17/2−)
375
172
599
(15/2−)
937
396
399
(11/2−)
110
(826)
228
116
713
(15/2−)
710
(13/2−)
524
521
189
11/2−